

CAMILA RODRIGUES BORGES LINHARES

A associação de oxigenoterapia hiperbárica e insulino-terapia favorece propriedades biomecânicas e reparo ósseo em ratos diabéticos

Hyperbaric oxygenation and insulin therapies association improves bone properties and repair in diabetic rats

Tese apresentada à Faculdade de Odontologia da Universidade de Uberlândia, para obtenção do Título de Doutor em Odontologia na Área de Clínica Odontológica Integrada.

Uberlândia, 2024

CAMILA RODRIGUES BORGES LINHARES

**A associação de oxigenoterapia hiperbárica e insulino-terapia favorece
propriedades biomecânicas e reparo ósseo em ratos diabéticos**

*Hyperbaric oxygenation and insulin therapies association improves bone properties and
repair in diabetic rats*

Tese apresentada à Faculdade de
Odontologia da Universidade de Uberlândia,
para obtenção do Título de Doutor em
Odontologia na Área de Clínica
Odontológica Integrada.

Orientadora: Profa. Dra. Paula Dechichi

Banca Examinadora:

Profa. Dra. Paula Dechichi

Profa. Dra. Camilla Christian Gomes Moura

Profa. Dra. Priscilla Barbosa Ferreira Soares

Prof. Dr. Gustavo Davi Rabelo

Profa. Dra. Virgínia Oliveira Crema

Uberlândia, 2024



UNIVERSIDADE FEDERAL DE UBERLÂNDIA

Coordenação do Programa de Pós-Graduação em Odontologia
Av. Pará, 1720, Bloco 4L, Anexo B, Sala 35 - Bairro Umuarama, Uberlândia-MG, CEP
38400-902

Telefone: (34) 3225-8115/8108 - www.ppgoufu.com - copod@umuarama.ufu.br



ATA DE DEFESA - PÓS-GRADUAÇÃO

Programa de Pós-Graduação em:	Odontologia				
Defesa de:	Tese, Doutorado, nº 97, PPGODONTO				
Data:	Vinte e Quatro de Junho de Dois Mil e Vinte e Quatro	Hora de início:	09:00	Hora de encerramento:	11:35
Matrícula do Discente:	12013ODO003				
Nome do Discente:	Camila Rodrigues Borges Linhares				
Título do Trabalho:	Associação de oxigenoterapia hiperbárica e insulino terapia favorece propriedades biomecânicas e reparo ósseo em ratos diabéticos				
Área de concentração:	Clínica Odontológica Integrada				
Linha de pesquisa:	Processo de Reparo				
Projeto de Pesquisa de vinculação:	Processo de Reparo				

Reuniu-se n o Anfiteatro/Sala 23 Bloco 4L - Anexo A Campus Umuarama, da Universidade Federal de Uberlândia, a Banca Examinadora, designada pelo Colegiado do Programa de Pós-graduação em Odontologia, assim composta: Professores Doutores: Virgínia Oliveira Crema (UFTM) participou da defesa de Tese por meio de vídeo conferência desde a cidade de Uberaba/MG; Gustavo Davi Rabelo (UFSC) participou da defesa de Tese por meio de vídeo conferência desde a cidade de Florianópolis/SC; Camilla Christian Gomes Moura (UFU); Priscilla Barbosa Ferreira Soares (UFU); Paula Dechichi Barbar (UFU); orientador(a) do(a) candidato(a).

Iniciando os trabalhos o(a) presidente da mesa, Dr(a). Paula Dechichi Barbar, apresentou a Comissão Examinadora e o candidato(a), agradeceu a presença do público, e concedeu ao Discente a palavra para a exposição do seu trabalho. A duração da apresentação do Discente e o tempo de arguição e resposta foram conforme as normas do Programa.

A seguir o senhor(a) presidente concedeu a palavra, pela ordem sucessivamente, aos(às) examinadores(as), que passaram a arguir o(a) candidato(a). Ultimada a arguição, que se desenvolveu dentro dos termos regimentais, a Banca, em sessão secreta, atribuiu o resultado final, considerando o(a) candidato(a):

Aprovado(a).

Esta defesa faz parte dos requisitos necessários à obtenção do título de Doutor.

O competente diploma será expedido após cumprimento dos demais requisitos,

conforme as normas do Programa, a legislação pertinente e a regulamentação interna da UFU.

Nada mais havendo a tratar foram encerrados os trabalhos. Foi lavrada a presente ata que após lida e achada conforme foi assinada pela Banca Examinadora.



Documento assinado eletronicamente por **Paula Dechichi Barbar, Professor(a) do Magistério Superior**, em 24/06/2024, às 11:37, conforme horário oficial de Brasília, com fundamento no art. 6º, § 1º, do [Decreto nº 8.539, de 8 de outubro de 2015](#).



Documento assinado eletronicamente por **Priscilla Barbosa Ferreira Soares, Professor(a) do Magistério Superior**, em 24/06/2024, às 11:37, conforme horário oficial de Brasília, com fundamento no art. 6º, § 1º, do [Decreto nº 8.539, de 8 de outubro de 2015](#).



Documento assinado eletronicamente por **Camilla Christian Gomes Moura, Professor(a) do Magistério Superior**, em 24/06/2024, às 11:37, conforme horário oficial de Brasília, com fundamento no art. 6º, § 1º, do [Decreto nº 8.539, de 8 de outubro de 2015](#).



Documento assinado eletronicamente por **Gustavo Davi Rabelo, Usuário Externo**, em 24/06/2024, às 11:44, conforme horário oficial de Brasília, com fundamento no art. 6º, § 1º, do [Decreto nº 8.539, de 8 de outubro de 2015](#).



Documento assinado eletronicamente por **VIRGÍNIA OLIVEIRA CREMA, Usuário Externo**, em 24/06/2024, às 11:48, conforme horário oficial de Brasília, com fundamento no art. 6º, § 1º, do [Decreto nº 8.539, de 8 de outubro de 2015](#).



A autenticidade deste documento pode ser conferida no site https://www.sei.ufu.br/sei/controlador_externo.php?acao=documento_conferir&id_orgao_acesso_externo=0, informando o código verificador **5483532** e o código CRC **1D454E91**.

Ficha Catalográfica Online do Sistema de Bibliotecas da UFU
com dados informados pelo(a) próprio(a) autor(a).

L755
2024

Linhares, Camila Rodrigues Borges, 1994-
Associação de oxigenoterapia hiperbárica e
insulinoterapia favorece propriedades biomecânicas e
reparo ósseo em ratos diabéticos [recurso eletrônico] :
Hyperbaric oxygenation and insulin therapies association
improves bone properties and repair in diabetic rats /
Camila Rodrigues Borges Linhares. - 2024.

Orientadora: Paula Dechichi.

Tese (Doutorado) - Universidade Federal de Uberlândia,
Pós-graduação em Odontologia.

Modo de acesso: Internet.

Disponível em: <http://doi.org/10.14393/ufu.te.2024.378>

Inclui bibliografia.

1. Odontologia. I. Dechichi, Paula ,1965-, (Orient.).

II. Universidade Federal de Uberlândia. Pós-graduação em
Odontologia. III. Título.

CDU: 616.314

Bibliotecários responsáveis pela estrutura de acordo com o AACR2:

Gizele Cristine Nunes do Couto - CRB6/2091
Nelson Marcos Ferreira - CRB6/3074

DEDICATÓRIA

Dedico este trabalho ao meu marido,
à minha mãe, à minha família
e aos meus amigos
que tanto amo, por todo amor,
carinho, paciência e apoio.

AGRADECIMENTOS

Ao atingir este objetivo da minha vida, não posso deixar de agradecer às pessoas que me apoiaram e fizeram parte de todo o meu processo de formação pessoal e acadêmica:

Agradeço à minha mãe **Cristina Rodrigues**, por todo cuidado, carinho, esforço, incentivo e sacrifícios que fez durante toda sua vida (os quais não foram poucos), para que eu pudesse estar aqui hoje. Ao olhar para trás e ver tudo que alcancei, sei que nada disso teria sido possível sem seu amor, apoio e sacrifícios. A ela, que é meu exemplo de força e perseverança, deixo aqui meu muito obrigada.

Agradeço ao meu marido **Igor Gonçalves**, que foi uma pessoa fundamental nesse processo, sendo meu melhor amigo, apoio, colo, ouvido, carinho, com muita paciência, e sempre me ajudando e incentivando a seguir em frente, sendo melhor e mais forte. Sem ele, a caminhada seria muito mais difícil.

Agradeço a minha prima **Marina Rodrigues**, a qual considero como uma irmã. Pela amizade, pelo companheirismo, por ser minha confidente, melhor amiga, por me apoiar, pelos conselhos, pelas risadas, e mesmo com toda distância que a vida impôs entre nós, por se fazer tão presente.

A meus familiares, em especial aos meus avós, a meu querido avô **José Rodrigues** (infelizmente já falecido) e a minha avó **Emirena Rodrigues**, pela excelente criação que me proporcionaram. Agradeço também as minhas tias **Mirela Rodrigues**, **Cristiane Rodrigues**, a minha Madrinha e tia **Marluce Rodrigues**, e ao meu irmão **Rodrigo Capanema**, por todo apoio, por serem uma extensão da minha casa, e por sempre acreditarem em mim.

A meus grandes amigos **Graziely**, **Leticia**, **Ester**, **Marisol**, **Yusmaris**, **Layane**, **Aline**, **Paulo** e **Marcelo**, pela amizade, companheirismo, apoio, pelas risadas, pela paciência, e por sempre me ajudarem e estarem comigo seja qual for a dificuldade.

Aos meus companheiros de grupo de pesquisa, **Maria Adelia, Marcelo Dias, e Pedro Limirio**. Por todo apoio, ajuda e companheirismo que tornaram o trabalho mais leve, agradável, e que muito contribuíram em minha formação durante todos esses anos.

Agradeço em especial a minha orientadora, **Profa. Dra. Paula Dechichi**, a qual eu tenho profunda admiração e gratidão por todo apoio durante todos esses anos. Sua dedicação incansável e paciência foram fundamentais para o meu desenvolvimento profissional e pessoal. Seu apoio foi essencial nos momentos em que me senti desafiada e suas palavras encorajadoras sempre me motivaram a seguir em frente. Cumprindo brilhantemente seu papel de orientadora, de forma humana, com muita paciência, dedicação e carinho. Sendo exemplo não somente como profissional, mas também como de ser humano.

AGRADECIMENTOS INSTITUCIONAIS

À Faculdade de Odontologia da Universidade Federal de Uberlândia (FOUFU) pelo apoio constante à pesquisa, ensino e extensão.

Ao Programa de Pós-Graduação da Faculdade de Odontologia da Universidade Federal de Uberlândia.

À Coordenação de Aperfeiçoamento de Pessoal de Nível Superior (CAPES) pela bolsa de estudos.

À Fundação de Amparo à Pesquisa de Minas Gerais (FAPEMIG), pelo financiamento desta pesquisa.

À Rede de Biotérios de Roedores da UFU (REBIR) da Universidade Federal de Uberlândia.

Ao Departamento de Biologia Celular, Histologia e Embriologia do Instituto de Ciências Biomédicas (ICBIM) da Universidade Federal de Uberlândia.

Aos professores da Faculdade de Odontologia da Universidade Federal de Uberlândia por todos os ensinamentos.

Aos funcionários do Laboratório de Histologia, Rede de Biotérios de Roedores (REBIR) e Centro de Pesquisa Odontológico Biomecânico, Biomateriais e Biologia Celular (CPBio) pelo apoio na parte experimental da pesquisa.

*“Não fique triste porque acabou, fique feliz
porque aconteceu.”*

Autor desconhecido

Sumário

RESUMO	12
ABSTRACT	13
1 - INTRODUÇÃO E REFERENCIAL TEÓRICO	14
2 - CAPÍTULOS	17
2.1 - Capítulo 1	17
2.2 - Capítulo 2	26
2.3 - Capítulo 3	47
3 – CONCLUSÃO	65
4 – REFERÊNCIAS*	66
5 – ANEXOS	73

RESUMO

O diabetes mellitus tipo 1 (DMT1) é uma doença metabólica caracterizada por hiperglicemia devido a alterações na secreção e/ou ação da insulina. A hiperglicemia crônica compromete o metabolismo, a estrutura e o reparo ósseo. Terapias adjuvantes, como a oxigenoterapia hiperbárica, têm sido propostas a fim de melhorar a estrutura e o reparo ósseo em condições desfavoráveis, como ocorre no DMT1. O objetivo do presente estudo foi avaliar os efeitos da oxigenoterapia hiperbárica associado à insulino terapia nas propriedades biomecânicas e reparo ósseo em rato com diabetes tipo I. Para isso, foram utilizados 48 ratos, distribuídos em seis grupos iguais. As análises utilizadas foram análise macroscópica, microtomografia computadorizada (MicroCT), espectroscopia no infravermelho transformada de Fourier (FTIR), teste de flexão em três pontos e histomorfometria à microscopia de luz. Além disso, utilizou-se o modelo de reparo ósseo para elaboração de um novo método de análise histomorfométrica de abordagem automática, comparando-o a métodos manual (padrão ouro) e semiautomatizado. Os resultados mostraram que a diabetes mellitus tipo I altera a microestrutura óssea, anisotropia e dimensão fractal, além de reduzir a espessura cortical e comprometer a composição e a dureza da matriz óssea. Os tratamentos combinados de oxigenoterapia hiperbárica e insulino terapia demonstraram reduzir esses efeitos adversos, sugerindo potencial terapêutico significativo para manejo de complicações ósseas em pacientes diabéticos. O método automatizado de análise histomorfométrica proposto, bem como os métodos manual e semiautomatizado foram eficazes para medir a formação óssea, sem diferenças estatísticas significativas entre eles. No entanto, a abordagem automática reduziu, significativamente, o tempo necessário para a análise, em comparação com os métodos manual e semiautomatizado. Concluiu-se que a associação das terapias com oxigenação hiperbárica e insulina diminui os efeitos negativos da hiperglicemia em ratos diabéticos, melhorando as propriedades e a regeneração ósseas. E, o método automatizado oferece uma avaliação rápida e precisa, com potencial para reduzir o viés e padronizar a análise histomorfométrica, sugerindo que essa técnica pode ser utilizada de forma confiável para quantificação da matriz óssea.

Palavras-chave: Análise automatizada; Regeneração óssea; Diabetes mellitus, Tipo I; Oxigenação hiperbárica

ABSTRACT

Type 1 diabetes mellitus (DMT1) is a metabolic disease characterized by hyperglycemia due to changes in insulin secretion and/or action. Chronic hyperglycemia compromises bone metabolism, structure, and repair. Adjuvant therapies, such as hyperbaric oxygen therapy, have been proposed to improve bone structure and repair in unfavorable conditions, as occurs in DMT1. The objective of the present study was to evaluate the effects of hyperbaric oxygen therapy associated with insulin therapy on biomechanical properties and bone repair in rats with type I diabetes. For this, 48 rats were used, distributed into six equal groups. The analyses used were macroscopic analysis, microcomputed tomography (MicroCT), Fourier transforms infrared spectroscopy (FTIR), three-point bending test, and histomorphometry under light microscopy. Furthermore, the bone repair model was used to develop a new histomorphometry analysis method with an automatic approach, comparing it to manual and semi-automated methods. The results showed that type I diabetes mellitus alters the bone microstructure, anisotropy and fractal dimension, in addition reduce cortical thickness and compromise the bone matrix composition and hardness. However, combined treatments of hyperbaric oxygen therapy and insulin therapy have been shown to reduce these adverse effects, suggesting significant therapeutic potential for managing bone complications in diabetic patients. The proposed automated method of histomorphometry analysis, as well as the manual and semi-automated methods, were effective in measuring bone formation, without significant statistical differences between them. However, the automatic approach significantly reduced the time required for analysis compared to manual and semi-automated methods. It was concluded that the association of therapies with hyperbaric oxygenation and insulin reduces the negative effects of hyperglycemia in diabetic rats, improving bone properties and regeneration. And, the automated method offers a fast and accurate assessment, with the potential to reduce bias and standardize histomorphometry analysis, suggesting that this technique can be used reliably to quantify bone matrix.

Keywords: Automated analysis; Bone regeneration; Diabetes mellitus Type I; Hyperbaric oxygenation; Insulin therapy

1 - INTRODUÇÃO E REFERENCIAL TEÓRICO

O Diabetes Mellitus tipo 1 (DMT1) é uma condição metabólica definida, principalmente, pela hiperglicemia, que resulta de deficiências na produção de insulina ou na sua função. Atualmente, cerca de 415 milhões de pessoas em todo o mundo são afetadas por essa doença, número que se prevê aumentar para 643 milhões até 2030, segundo a International Diabetes Federation (2021). O diabetes tipo 1 é identificado como uma doença autoimune que danifica as células β do pâncreas, que produzem insulina, podendo ou não restar tecido funcional. As origens do diabetes tipo 1 são variadas, incluindo fatores como infecções virais, efeitos colaterais de medicamentos e reações autoimunes, que resultam na morte celular e subsequente deficiência de insulina, elevando os níveis de glicose no sangue (Wang et al., 2017).

A hiperglicemia crônica ocasionada pela DMT1 altera negativamente a microarquitetura e as propriedades biomecânicas do tecido ósseo (Ay et al., 2020; Limirio et al., 2024). Além disso, o DMT1 compromete a reparação óssea, aumenta o risco de fraturas (Bai et al., 2020; Starup-Linde et al., 2016) e está relacionado a maiores taxas de complicações durante procedimentos cirúrgicos (Martin et al., 2016). Estudos sugerem que o comprometimento ósseo é devido ao excesso de produtos de glicação avançada (AGEs) no sangue e sua incorporação no tecido ósseo (Yang et al., 2015). A acumulação de AGEs nos ossos interfere na qualidade da matriz e na diferenciação e função das células ósseas (Yang et al., 2015).

Atualmente, a terapia com insulina é o tratamento de escolha para pacientes com DMT1. Seu uso é capaz de reduzir os níveis de glicose no sangue e permitir que sejam controlados. Estudos recentes mostram que pacientes com DMT1 com glicemia controlada são significativamente menos afetados pelos efeitos deletérios no tecido ósseo em suas propriedades biomecânicas e microarquitetura (Limirio et al., 2024) e nas taxas de densidade mineral (Susuki et al., 2022). Além do seu papel na regulação da glicose, a insulina tem sido reconhecida pelo seu impacto na saúde óssea. Os receptores de insulina estão presentes nos osteoblastos e osteoclastos, indicando uma influência direta no metabolismo ósseo (Thraillkill et al., 2005). Além disso, foi demonstrado que a insulina estimula a produção de fatores de crescimento como o fator de crescimento semelhante à

insulina 1 (IGF-1), que é essencial para o crescimento e reparação óssea (Thraillkill et al., 2005).

Novas terapias têm sido investigadas e propostas para melhorar o processo de reparação óssea, especialmente em condições desfavoráveis, como o diabetes. A terapia de oxigenação hiperbárica ganhou reconhecimento por seu potencial em aprimorar a reparação óssea (Dias et al., 2018), melhorar a microcirculação (Mathieu et al., 2006), e reduzir a inflamação (Benson et al., 2003). Essa terapia consiste na oferta de oxigênio puro (100%) em um ambiente pressurizado a um nível acima da pressão atmosférica.

Estudos relataram que a oxigenação hiperbárica aumenta a quantidade de oxigênio no sangue e promove a angiogênese em tecidos lesionados, aumentando a quantidade de oxigênio e nutrientes no local lesionado (Jan et al., 2009), acelerando o processo de reparação em tecidos moles (Kalani et al., 2002) e tecidos mineralizados (Rocha et al. 2015; Dias et al. 2018). No tecido ósseo, a oxigenação hiperbárica mostrou melhorias nas propriedades mecânicas ósseas, aumentando a força e rigidez do fêmur em animais com DMT1 (Limirio et al. 2018). Um estudo de Kawada e colaboradores (2013) demonstrou que essa terapia, em camundongos saudáveis, aumenta a taxa de aposição mineral óssea e interfere positivamente na reabsorção do calo ósseo e na consolidação de fraturas, acelerando o processo de remodelação óssea nesta situação.

Os efeitos específicos da terapia de oxigênio hiperbárico e da terapia de insulina nos ossos de pacientes com DMT1 não são completamente compreendidos. O uso combinado de oxigenação hiperbárica e terapia com insulina pode oferecer uma abordagem sinérgica. A oxigenação hiperbárica fornece o suporte de oxigênio necessário para as atividades celulares envolvidas na reparação óssea, enquanto a terapia com insulina visa o equilíbrio metabólico subjacente associado ao diabetes. O presente estudo contribui para o entendimento de como essas terapias interferem nas características e propriedades mecânicas dos ossos.

Além disso, a quantificação precisa de eventos biológicos é crucial para a avaliação dos efeitos das terapias e da condição sistêmica, especialmente em doenças. A análise histomorfométrica é frequentemente usada para avaliar parâmetros histológicos. As ferramentas computacionais utilizadas em imagens digitalizadas ou o método de contagem com um observador treinado (através de análise visual) são bastante comuns

em análises histológicas qualitativas e quantitativas (Mendes et al., 2020; Soares et al., 2019). Geralmente, o método tradicional de análise histológica demanda um longo tempo de análise e depende significativamente da experiência do operador, o que pode ocasionar viés no processo analítico.

Com os avanços tecnológicos, os sistemas de análises automatizadas têm sido estudados para sua aplicação na avaliação de imagens histológicas. Esses sistemas permitem a análise de um maior número de imagens em um tempo reduzido. Além disso, as análises automatizadas podem aumentar a eficiência e precisão do processo analítico, sendo semelhantes ao método tradicional de análise, realizada por um observador experiente (padrão ouro) (Gonzalez & Madeiras, 2018; Hammes et al., 2018; Steiner et al., 2018).

O objetivo do presente estudo foi avaliar o efeito da associação da oxigenoterapia hiperbárica e da insulinoterapia na microarquitetura, composição química, propriedades mecânicas e a reparação óssea em ratos com Diabetes Mellitus Tipo I. Além disso, propor um método automatizado de análise histomorfométrica para quantificação da matriz óssea, comparando-o com métodos convencionais. A hipótese do estudo foi que a associação das terapias com oxigenação hiperbárica e insulina afeta positivamente a microarquitetura, a composição da matriz, a propriedades biomecânicas dos ossos e reparação óssea em ratos com DMT1. Assim, essas intervenções juntas poderiam ter o potencial de eliminar as consequências do DMT1 e tornar a estrutura óssea similar à de ratos normoglicêmicos. Também, hipotetizou-se que o método automatizado de análise histomorfométrica de matriz óssea apresenta maior precisão e menor tempo de análise, comparado a métodos convencionais.




2 - CAPÍTULOS

2.1 - Capítulo 1

Linhares CRB, Rabelo GD, Limirio PHJO, Venâncio JF, Silva IGRS, Dechichi P. Automated bone healing evaluation: New approach to histomorphometric analysis. Microsc Res Tech. 2022;85(10):3339-46.

DOI: [10.1002/jemt.24188](https://doi.org/10.1002/jemt.24188)

Automated bone healing evaluation: New approach to histomorphometric analysis

Camila Rodrigues Borges Linhares¹ | Gustavo Davi Rabelo²  |
Pedro Henrique Justino Oliveira Limirio¹  | Jessyca Figueira Venâncio¹ |
Igor Gonçalves Ribeiro Silva³ | Paula Dechichi⁴ 

¹Dentistry Department, Federal University of Uberlândia, Uberlândia, Minas Gerais, Brazil

²Dentistry Department, Federal University of Santa Catarina, Florianópolis, Santa Catarina, Brazil

³Department of Electrical Engineering, Federal University of Uberlândia, Uberlândia, Minas Gerais, Brazil

⁴Department of Cell Biology, Histology and Embryology, Biomedical Science Institute, Federal University of Uberlândia, Uberlândia, Minas Gerais, Brazil

Correspondence

Paula Dechichi, Department of Cell Biology, Histology and Embryology, Biomedical Science Institute, Federal University of Uberlândia, Bairro Umuarama, Uberlândia, Minas Gerais 38.405-318, Brazil.
Email: pauladechichi@ufu.br

Funding information

Research Support Foundation of the State of Minas Gerais (FAPEMIG/Brazil), Grant/Award Number: 001; Coordenação de Aperfeiçoamento de Pessoal de Nível Superior – Brasil (CAPES), Grant/Award Number: APQ-02003-14

Review Editor: Paul Verkade

Abstract

This study aimed to assess different approaches for bone healing evaluation on histological images and to introduce a new automatic evaluation method based on segmentation with distinct thresholds. We evaluated the hyperbaric oxygen therapy (HBO) effects on bone repair in type 1 diabetes mellitus rats. Twelve animals were divided into four groups ($n = 3$): non-diabetic, non-diabetic + HBO, diabetic, and diabetic + HBO. Diabetes was induced by intravenous administration of streptozotocin (50 mg/kg). Bone defects were created in femurs and HBO was immediately started at one session/day. After 7 days, the animals were euthanized, femurs were removed, demineralized, and embedded in paraffin. Histological sections were stained with hematoxylin and eosin (HE) and Mallory's trichrome (MT), and evaluated using three approaches: (1) conventional histomorphometric analysis (HE images) using a 144-point grid to quantify the bone matrix; (2) a semi-automatic method based on bone matrix segmentation to assess the bone matrix percentage (MT images); and (3) automatic approach, with the creation of a plug-in for ImageJ software. The time required to perform the analysis in each method was measured and subjected to Bland–Altman statistical analysis. All three methods were satisfactory for measuring bone formation and were not statistically different. The automatic approach reduced the working time compared to visual grid and semi-automated method ($p < .01$). Although histological evaluation of bone healing was performed successfully using all three methods, the novel automatic approach significantly shortened the time required for analysis and had high accuracy.

KEYWORDS

automated image analysis, bone regeneration, computer-assisted, hyperbaric oxygenation, type 1 diabetes mellitus

Highlights

- A new automatic evaluation method based on segmentation with distinct thresholds.
- The method proposed was significantly shortened the time required for analysis.
- The automatic approach analysis had high accuracy.

1 | INTRODUCTION

Precise quantification of biological events is crucial for the evaluation of drug effects and systemic conditions, especially in diseases. Histomorphometric analysis is often used to analyze and compare groups under experimental conditions and assess histological parameters. The computational tools used in digitized images or the counting method with a trained observer (through visual analysis) are quite common when using microscopic qualitative and quantitative evaluations (Mendes et al., 2020; Soares et al., 2019). Generally, the traditional histological analysis method has a lengthy analysis time and depends significantly on the operator's experience, which can introduce bias in the analytical process.

With technological advances, computer-aided analysis systems have been studied for their application in the evaluation of histological images. These tools are called computer-aided diagnosis (CAD) and enable analysis through an automated approach using computational algorithms. These systems allow the analysis of large images, in significantly greater numbers, in a shorter time, thereby reducing the time required for analysis. In addition, they may increase the efficiency and accuracy of the analytical process, which is usually similar to the visual analysis performed by an experienced observer (Gonzalez & Woods, 2018; Hammes et al., 2018; Steiner et al., 2018).

Several studies have used the counting method with trained observers in digital images to analyze tissue repair, especially bone healing and remodeling under adverse conditions (Batista et al., 2015; Dias et al., 2018; Rocha et al., 2016). However, there is a lack of studies that present an automated approach to analyze the bone matrix.

The present study compared the conventional methods and to proposed a new one based on total automation, using a well-known experimental method for bone repair analysis. Therefore, for the analysis of the new methodology we used an experiment model of rats with type I diabetes mellitus (T1DM) and hyperbaric oxygenation (HBO) therapy, that has been used successfully to evaluate bone healing by histological analysis (Dias et al., 2018). T1DM is a metabolic disease (Wang et al., 2019) that causes hyperglycemia (Napoli et al., 2017; Palermo et al., 2017) which affects bone structure and repair (Nyman et al., 2011). HBO therapy has been suggested as an adjuvant therapy to improve and accelerate bone regeneration (Dias et al., 2018; Limirio et al., 2018; Rocha et al., 2016).

Results obtained from the experimental model, the present study aimed to compare three different methods of histological evaluation of bone repair: (1) a conventional visual evaluation through histomorphometric analysis, using a 144-points grid to quantify the bone matrix; (2) a semi-automatic method based on the segmentation of bone matrix from the soft tissue, to assess the total bone matrix percentage; and (3) an automatic approach, developed in this study, through the creation of a plug-in for ImageJ software, including distinct steps for image processing and a thresholding binarization for the bone matrix. The hypothesis was that automated image analysis using a computer-aided analysis system can present greater precision and less time consumed compared to visual quantitative analysis performed by an experienced observer.

2 | MATERIAL AND METHODS

2.1 | Study design

All experimental protocols involving animals were approved by the Committee on the Ethics of Animal Use and Care of the Federal University of Uberlândia (permit number 026/14). Twelve male Wistar rats (*Rattus norvegicus*) weighing 240 ± 20 g at the age of 8 weeks were housed under standard conditions. After 1 week of acclimatization, the animals were randomly assigned and equally distributed into the following four groups ($n = 3$): non-diabetic (N), non-diabetic + HBO (NH), diabetic (D), and diabetic + HBO (DH). TDMI induction, follow-up evaluation, glycemic assessment, surgical procedure, and HBO therapy were performed as described by Dias et al. (2018), the only change made was in the induction dosage (50 mg/kg). All animals were euthanized 37 days after diabetes induction, the femurs were dissected, the epiphyses were removed, and the diaphyses were immediately fixed in 4% paraformaldehyde solution in phosphate-buffered saline for 48 h. Subsequently, the diaphyses were decalcified in 4.13% EDTA for 5 weeks and embedded in paraffin. Six semi-serial histological sections (5 μm) were obtained from each animal: three in hematoxylin–eosin (HE) and three in Mallory's trichrome (MT). All histological sections were scanned using the Aperio AT Turbo Scanner (Leica Biosystems Imaging, Inc. Nußloch, Germany) at 20 \times magnification. The digitized histological images were visualized using the Aperio ImageScope imaging program and exported as TIFF files.

The digital histological images containing the bone defect were analyzed by the counting method by a trained observer using the point grid, semi-automated, and automated image analysis methods.

2.2 | Histological quantitative method—visual analysis with point grid

Histological images stained with HE were used for visual analysis, using a point grid performed by an experienced observer. The analysis was performed using Image-Pro Plus software (Version 4.5.0.29; Media Cybernetic, Inc., Rockville, MD), with a 144-point grid positioned over the selected areas containing the new bone. In summary, from the region of interest (ROI) at the bone defect, three areas were extracted for analysis with the grid, two near the cortical disruption, and one at the clot (Figure 1a). Each area selected was transformed into an image in TIFF format, with an area of $431 \times 431 \mu\text{m}^2$ (Figure 1b). After calibration (association of the number of pixels in the image with real measurements of the physical world), the 144-point grid was overlaid, and each point corresponding to the bone was marked in pink. The bone matrix was manually marked and then quantified and expressed as percentages. Point counting was performed by the same operator who was blinded to the groups. Any disagreements between the two examiners were resolved by a third examiner. The inter-reviewer reliability of data extraction was calculated by determining the percentage of agreement and the correlation coefficient (kappa, 5% level of significance).

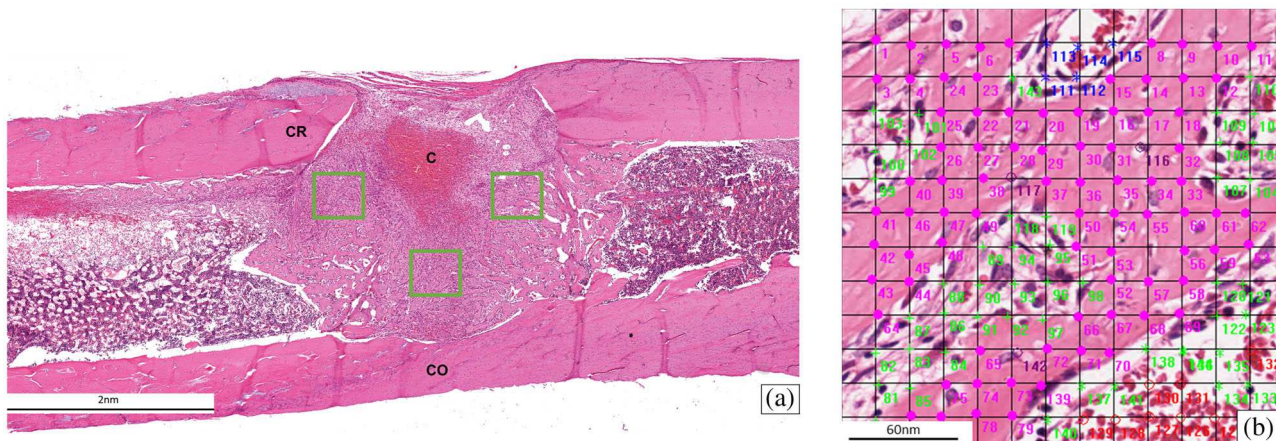


FIGURE 1 (a) Histological image (stained with hematoxylin and eosin, HE) of a longitudinal section of the femur in the bone lesion area, showing ruptured cortical (CR), opposite cortical (CO), clot (C), bone neoformation region (*), and select areas (green squares). (b) Image generated by the image-pro plus software, illustrating the grid of points (bone matrix: Pink; marrow: Green; blood vessel: Blue) on the histological image used for bone matrix quantification

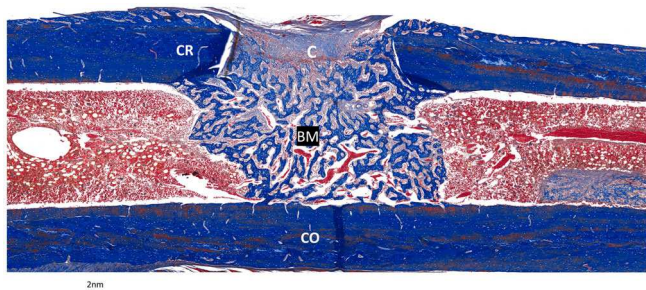


FIGURE 2 Histological image (stained with Mallory's trichrome, MT) of a longitudinal section of the femur in the bone defect area, showing the disrupted cortex (CR), the opposite cortical (CO), the clot (C), and the bone neoformation (BM)

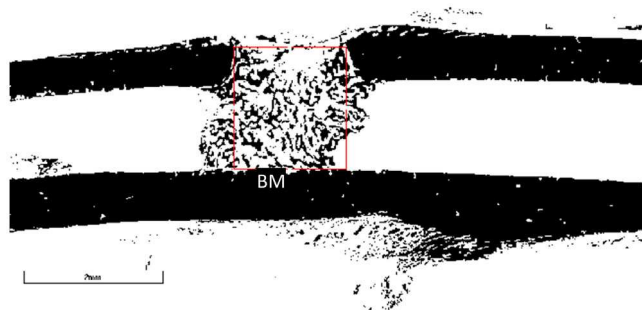


FIGURE 3 A digitized histological image of a longitudinal section of the diaphysis of the femur after soft tissue was removed. The binary image reveals the region of interest (red rectangle), showing the disrupted cortex (CR), the opposite cortical (CO), the clot (C), and the bone neoformation region (BM)

2.3 | Histological semi-automated image analysis (computer-assisted)

A semi-automated computer-assisted method was performed in the histological sections stained with MT to quantify bone neoformation, as a percentage (Figure 2). Digital images were uploaded to Adobe Photoshop CS6 (Adobe System Inc., San Jose, CA) image editor software for soft tissue removal. Using the ImageJ software (Version 1.53a; National Institutes of Health, Bethesda, MD), the images were converted into binary images and the ROI was delimited by four lines, extending from the edges of the cortical bone to the opposite cortical, using the draw tool (Figure 3) (Batista et al., 2015; Dias et al., 2018). The percentage of neoformed bone matrix within the ROI was calculated using the measurement tool. Binarization and thresholding were performed by the same operator who was blinded to the groups.

2.4 | Histological automated image analysis (computer-assisted)

Histological images stained with HE were used for this analysis, through the assessment and segmentation of the bone matrix, followed by quantification (as a percentage). A plug-in to be used in the ImageJ software was created using the following well-defined sequence of steps to evaluate the bone matrix.

1. Calibration of the scale.
2. Conversion of the image to 8 bit.
3. Adjustment of the contrast and saturation, followed by normalization and equalization of the image.
4. Quantification of bone matrix defined using a threshold interval of 158–215.
5. Generation of results (doc) with the percentage of pixels within the binary image.

The thresholding interval used for segmentation was defined through the analysis of all images, with the definition of a global threshold that fitted in all images. The programming language Java was used to write the code. The files were saved in .java format and compiled, generating the .class file, which was installed in ImageJ.

The algorithm and code for the plug-in that was created, is accessible on GitHub at <https://github.com/igorgonribs/imagej-plugin-histology-ufu/tree/main> and in the supplementary material.

2.5 | Measurement of analytical time

The time consumed for each method was measured in seconds, and a comparison of the time spent on each of the three methods was performed.

2.6 | Statistical analysis

Statistical analysis was performed using Sigma Plot (Version 13.1; Systat Software Inc, San Jose, CA) statistical software. The results obtained were subjected to the Kolmogorov–Smirnov normality test, followed by the two-way ANOVA and finally the Tukey test. Results are presented as mean \pm standard deviation (SD). Differences were considered to be statistically significant at $\alpha < 0.05$.

The PASW Statistics software (Version 18.0.0; SPSS Ltd Software Inc, Quarry Bay, Hong Kong) was used for agreement verification among the methods. The results obtained were subjected to Bland–Altman analysis and subsequently to the regression linear test for verification of proportion bias (the tendency for values to be above or below the average). Results are presented as mean bias \pm standard

deviation (SD), and the upper and lower limits of agreement are presented as mean $\pm 1.96 \times$ SD. Statistical agreement was considered at $\alpha > 0.05$.

3 | RESULTS

Throughout the experimental procedure, the diabetic animals (D and DH) maintained hyperglycemia (glucose levels above 300 mg/dl), weight reduction, polyphagia, polydipsia, and polyuria, observed from the increase in feed and water intake, and urinary excretion. The success rate of diabetes induction in animals was 95% and mortality was less than 10%. The mean and standard deviation values for the glucose level are shown in Table 1. The mean glycemiac index of total periods showed that N and NH had lower glycemia than D and DH, respectively (Figure 4a). There were increase glucose level in the D group ($p < .01$) compared 30–37 days, however, the DH group ($p < .01$) decrease glucose level compared the periods of 30–37 days (Figure 4b).

The histomorphometric results are shown in Table 2. The bone matrix analysis in HE (Figure 5a) and MT (Figure 5b) stains showed that group D had lower values than groups N and DH ($p < .01$). The bone matrix automated method (Figure 5c) revealed similar grad point visual analysis.

3.1 | Bland–Altman analysis results

The Bland–Altman analysis showed that the visual method and semi-automated image analysis method also displayed strong agreement. The mean difference between the visual method and automated

TABLE 1 The means and standard deviation values of glucose level

Glucose level (mg/dl)/groups	Non-diabetic (N)	Non-diabetic + HBO (NH)	Diabetic (D)	Diabetic + HBO (DH)
Day 0	96.1 \pm 6.7	96.5 \pm 6.4	333.2 \pm 26.3	313.6 \pm 50.4
Day 15	97.2 \pm 11.8	97.6 \pm 7.3	322.5 \pm 16.3	541.0 \pm 67.8
Day 30	96.8 \pm 5.7	100.4 \pm 11.8	416.0 \pm 9.1	549.0 \pm 69.3
Day 37	92.2 \pm 10.47	83.4 \pm 6.18	558.33 \pm 39.2	270.0 \pm 46.2
Total mean	95.6 \pm 2.3	94.4 \pm 7.5	332.5 \pm 22.8	419.1 \pm 146.6

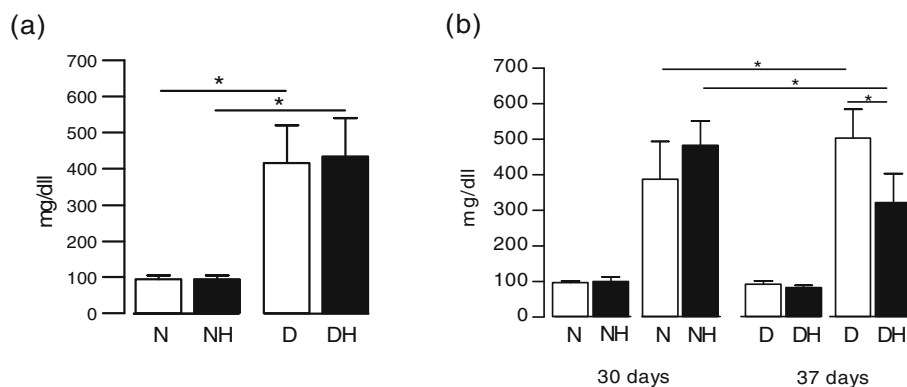


FIGURE 4 Glucose values analysis in the different groups. $*p < .05$. (a) Glucose level/(b) glucose level 30 \times 37 days/non-diabetic – N/non-diabetic + HBO – NH/diabetic – D/diabetic + HBO – DH

TABLE 2 Histomorphometric results

Parameters/groups	Non-diabetic (N)	Non-diabetic + HBO (NH)	Diabetic (D)	Diabetic + HBO (DH)
Bone matrix (visual analysis)	36.7 ± 1.1 ^{Aa}	36.8 ± 1.2 ^{Aa}	28.3 ± 2.7 ^{Bb}	36.2 ± 1.5 ^{Aa}
Bone matrix (semi automated analysis)	24.1 ± 2.4 ^{Aa}	26.1 ± 1.1 ^{Aa}	14.7 ± 3.7 ^{Bb}	22.0 ± 3.6 ^{Aa}
Bone matrix (automated image analysis)	28.31 ± 0.97 ^{Aa}	32.93 ± 3.85 ^{Aa}	26.51 ± 3.18 ^{Aa}	33.84 ± 1.42 ^{Bb}

Note: The mean and SD values of histomorphometric analysis in the bone regeneration area. In the rows, different capital letters indicate significant differences for diabetic factors (N and NH groups vs. D and DH groups), and different lowercase letters indicate significant differences for hyperbaric oxygen therapy (N and D vs. NH and DH) ($p < .05$).

FIGURE 5 Histomorphometric analysis of the parameters in the different groups (* $p < .05$). (a) Histomorphometric results of histological bone matrix visual image analysis. (b) Histomorphometric results of histological semi-automated image analysis. (c) Histomorphometric results of histological automated image analysis

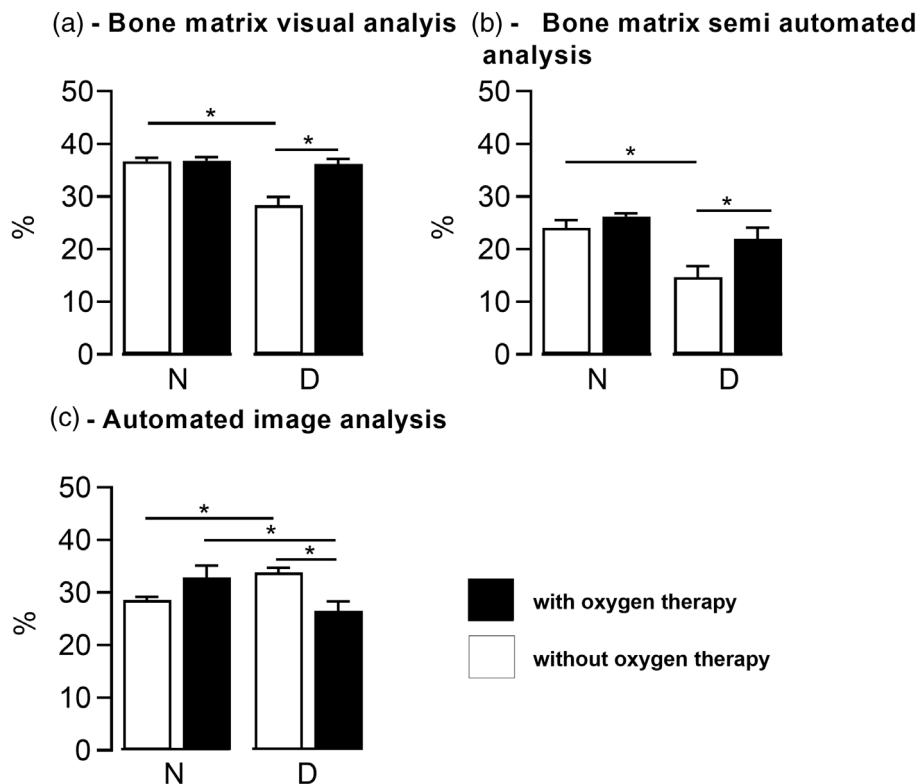


image analysis method for bone matrix quantification was -12.78 ± 2.70 , and the limits of agreement were -18.07 and -7.49 , respectively. No statistically significant difference was estimated by these two methods ($p = .10$), and no proportion bias tendency was seen in the regression linear results. The p -value of the averages was $p = .16$ (Figure 6a).

The Bland-Altman analysis demonstrated that the visual method and automated image analysis method displayed strong agreement. The mean difference between the visual method and automated image analysis method for bone matrix quantification was -4.07 ± 6.56 , and the limits of agreement were 8.79 and -16.93 , respectively. No statistically significant difference was estimated by these two methods ($p = .055$), and no proportion bias tendency (there was no tendency for values to be above or below average) was seen in the

regression linear results. The p -value of the averages was $.89$ (Figure 6b).

3.2 | Assessment of the analytical time and the accuracy of the methods

The time consumed analysis, showed a significant statistically difference (* $p < .001$) between groups automated, visual, and semi-automated method. The automated method (0.08 ± 0.0 , seconds) had significantly lower values than the visual method (904.67 ± 3.77) and semi-automated method (303.33 ± 2.99).

The mean accuracy was $83.84 \pm 7.20\%$ for the automated method compared with the visual analysis method. The accuracy

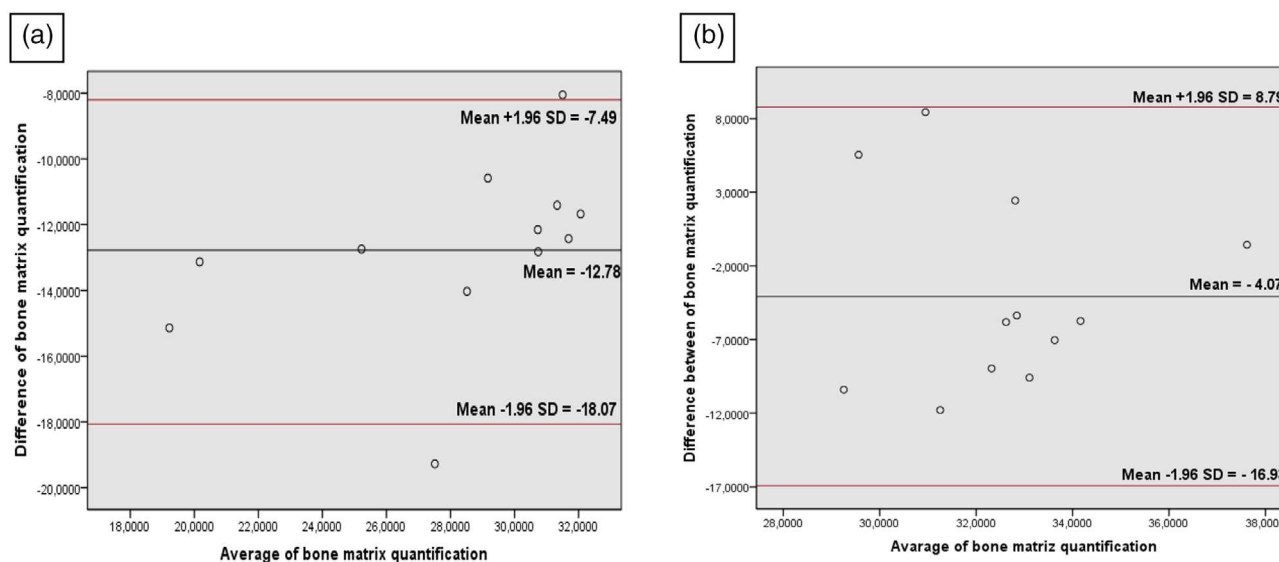


FIGURE 6 (a) Agreement between visual and semi-automated methods (Bland–Altman plot). (b) Agreement between visual and automated methods (Bland–Altman plot)

calculated for the semi-automated method with the visual analysis method was $68.15 \pm 4.41\%$.

4 | DISCUSSION

The hypothesis of this study was confirmed since the automated computer-assisted method resulted in similar findings as the visual-manual method while showing a significant reduction in the time spent on the histological evaluation process. The automated method showed significant agreement with the visual method, also revealing high accuracy (high precision of the results and low risk of error), with the possibility of standardization, together with a reduction in working time and biases in the analysis process. Taking these results into account, it is suggested that researchers who have been trying to improve their analysis for the diagnosis and quantification of bone matrix could benefit from the proposed automated method.

Regarding the automatization of histological evaluation, some methods are being developed using more sophisticated algorithms, such as those used in artificial intelligence. Methods such as machine learning and its sub-methods such as neural networks and deep learning (Hammes et al., 2018; Jones et al., 2009; Lamprecht et al., 2007; Silva et al., 2019) have been studied with promising results. Nevertheless, there are simple methods that are more democratic, based on the use of software and plug-ins, available in the public domain and are free of charge. One such free software program is ImageJ, which is available from the National Institutes of Health. Several plug-ins related to segmentation tools are available for use in all images, including all histological figures (Schindelin et al., 2015). Segmentation using a threshold was sufficient to create an automated method in this study, together with other image processing steps, which allowed for the creation of a plug-in for bone formation/repair evaluation

(Schindelin et al., 2015). Plug-ins and macros can be implemented using the ImageJ software (Reyes-Fernandez et al., 2019). In addition, previous studies using semi-automated methods have already assessed segmentation by thresholding, but without automatization (Batista et al., 2015; Dias et al., 2018; Rocha et al., 2016). The automatization in this study was not just created but also tested, and the resulting significant reduction in the time of analysis was encouraging.

Automated methods are of great importance in microscopic analysis and are useful tools (Batista et al., 2015; Gonzalez & Woods, 2018; Hammes et al., 2018). The results obtained by automatization demonstrated the advantage of reducing the time required for analysis by 11,250X, while maintaining high accuracy (83.84%), when compared with the visual analysis performed by an experienced observer, and by 3750X when compared with the semi-automated method. In addition, all methods displayed strong agreement, presenting similar results. It was observed that there is no difference in the significance between the three types of analysis, and similar results to this study were demonstrated in the literature using different experimental conditions (Reyes-Fernandez et al., 2019; Tamminga et al., 2016), confirming that the automated and semi-automated method proposed can be used reliably.

In addition to the developed method, our findings on the effects of HBO on the initial bone repair process in animals with normoglycemia and diabetes are consistent with previous studies (Dias et al., 2018; Okubo et al., 2001; Rocha et al., 2016; Wu et al., 2007) and increased the knowledge about this adjuvant therapy in the literature concerning bone healing improvement. The results presented in this animal experimental study, together with other human studies, suggest that HBO therapy is a safe and valuable strategy that could be used to enhance and improve regenerative clinical therapies, especially in conditions with alterations in bone metabolism, such as diabetes (Dias et al., 2018; Rocha et al., 2016).

In the present study, diabetic animals submitted to HBO therapy showed decrease glucose levels after the surgery. T1DM substantially reduces the number of pancreatic β cells, but the remaining cells still have some degree of function (Fotino et al., 2013; Prabowo et al., 2014). Some studies have shown that use an appropriate protocols of HBO therapy can significantly decrease oxidative stress and reduced reactive oxygen species (ROS) production, which reduced apoptosis and increased proliferation of β -cells (Faleo et al., 2012; Fotino et al., 2013; Rajagopalan et al., 2012; Prabowo et al., 2014). Thus, the increase insulin production reduce glycemic levels, approaching the normality systemic condition (Lu et al., 2008).

In addition to the creation of the automatized method for histological evaluation, this study aimed to create a tool that was easily accessible, improving the popularization of the use of this and other segmentation tools and was also easy to install in ImageJ. The use of public domain software should be encouraged to improve and democratize microscopic analysis tools for researchers worldwide.

4.1 | Limitations

The limitations of the proposed automated method should be discussed. The global threshold for all images and the process of segmentation produce some issues, such as the loss of information (Kim et al., 2018; Reyes-Fernandez et al., 2019; Tamminga et al., 2016). Therefore, it is necessary to conduct more studies on automatization applications in microscopic analysis for the improvement of segmentation tools. The plug-in proposed in this study works well in some conditions, with specific staining, usage of good quality images, and an adequate background. The data should not be extrapolated to other stains without calibration and adjustment of the Java programming features.

5 | CONCLUSION

The automated computer-assisted method for histological evaluation achieved similar results to the visual-manual method while presenting some benefits concerning standardization and reduced analysis time. All three methods used (visual-manual, semi-automated, and automated) for histological evaluation were successful in bone matrix analysis. The automated method demonstrated high accuracy, suggesting that this method should be encouraged under experimental conditions to evaluate the bone repair process.

AUTHOR CONTRIBUTIONS

Camila Rodrigues Borges Linhares: design of the work, acquisition and tabulation and analysis of data, code development, creation of tables and figures, drafting of the text. **Gustavo Davi Rabelo:** design of the work, revising critically for important intellectual content and addition of significant parts. **Igor Gonçalves Ribeiro Silva:** design of the work, code development, drafting of the text. **Jessyca Figueira Venâncio:** design of the work, revising critically for important

intellectual content and addition of significant parts. **Paula Dechichi:** design of the work, revising it critically for important intellectual content and addition of significant parts. **Pedro Henrique Justino Oliveira Limirio:** conception and design of the work, revising it critically for important intellectual content and addition of significant parts.

ACKNOWLEDGMENTS

The authors are grateful to the Institute of Biomedical Sciences (ICBIM), the Network of Animal Facilities (REBIR) and the Research Center in Biomechanics, Biomaterials and Dental Cell Biology (CPBIO) of the Federal University of Uberlândia.

FUNDING INFORMATION

This work was supported by Coordenação de Aperfeiçoamento de Pessoal de Nível Superior – Brasil (CAPES) – Finance Code 001 and Research Support Foundation of the State of Minas Gerais (FAPEMIG/Brazil) APQ-02003-14.

CONFLICT OF INTEREST


The authors declare no potential conflict of interest.

DATA AVAILABILITY STATEMENT

The algorithm and code for the plug-in that was created, is accessible on GitHub at <https://github.com/igorgonribs/imagej-plugin-histology-ufu/tree/main>.

ORCID

Gustavo Davi Rabelo  <https://orcid.org/0000-0001-9511-5078>

Pedro Henrique Justino Oliveira Limirio  <https://orcid.org/0000-0002-0089-3772>

Paula Dechichi  <https://orcid.org/0000-0001-5509-8138>

REFERENCES

- Batista, J. D., Sargenti-Neto, S., Dechichi, P., Rocha, F. S., & Pagnoncelli, R. M. (2015). Low-level laser therapy on bone repair: Is there any effect outside the irradiated field? *Lasers in Medical Science*, 30(5), 1569–1574. <https://doi.org/10.1007/s10103-015-1752-3>
- Dias, P. C., Limirio, P., Linhares, C. R. B., Bergamini, M. L., Rocha, F. S., Morais, R. B., Balbi, A. P. C., Hiraki, K. R. N., & Dechichi, P. (2018). Hyperbaric oxygen therapy effects on bone regeneration in type 1 diabetes mellitus in rats. *Connective Tissue Research*, 59(6), 574–580. <https://doi.org/10.1080/03008207.2018.1434166>
- Faleo, G., Fotino, C., Bocca, N., Molano, R. D., Zahr-Akrawi, E., Molina, J., Villate, S., Umland, O., Skyles, J. S., Bayer, A. L., Ricordi, C., & Pileggi, A. (2012). Prevention of autoimmune diabetes and induction of beta-cell proliferation in NOD mice by hyperbaric oxygen therapy. *Diabetes*, 61(7), 1769–1778. <https://doi.org/10.2337/db11-0516>
- Fotino, C., Molano, R. D., Ricordi, C., & Pileggi, A. (2013). Transdisciplinary approach to restore pancreatic islet function. *Immunologic Research*, 57(1–3), 210–221. <https://doi.org/10.1007/s12026-013-8437-4>
- Gonzalez, R. C., & Woods, R. E. (2018). *Digital image processing*. Pearson.
- Hammes, J., Tager, P., & Drzezga, A. (2018). EBONI: A tool for automated quantification of bone metastasis load in PSMA PET/CT. *Journal of Nuclear Medicine*, 59(7), 1070–1075. <https://doi.org/10.2967/jnumed.117.203265>
- Jones, T. R., Carpenter, A. E., Lamprecht, M. R., Moffat, J., Silver, S. J., Grenier, J. K., Castoreno, A. B., Eggert, U. S., Root, D. E., Golland, P., &

- Sabatini, D. M. (2009). Scoring diverse cellular morphologies in image-based screens with iterative feedback and machine learning. *Proceedings of the National Academy of Sciences of the United States of America*, 106(6), 1826–1831. <https://doi.org/10.1073/pnas.0808843106>
- Kim, J. J., Nam, J., & Jang, I. G. (2018). Fully automated segmentation of a hip joint using the patient-specific optimal thresholding and watershed algorithm. *Computer Methods and Programs in Biomedicine*, 154, 161–171. <https://doi.org/10.1016/j.cmpb.2017.11.007>
- Lamprecht, M. R., Sabatini, D. M., & Carpenter, A. E. (2007). CellProfiler: Free, versatile software for automated biological image analysis. *Bio-Techniques*, 42(1), 71–75. <https://doi.org/10.2144/000112257>
- Limirio, P., da Rocha Junior, H. A., Morais, R. B., Hiraki, K. R. N., Balbi, A. P. C., Soares, P. B. F., & Dechichi, P. (2018). Influence of hyperbaric oxygen on biomechanics and structural bone matrix in type 1 diabetes mellitus rats. *PLoS One*, 13(2), e0191694. <https://doi.org/10.1371/journal.pone.0191694>
- Lu, M. P., Wang, R., Song, X., Chibbar, R., Wang, X., Wu, L., & Meng, Q. H. (2008). Dietary soy isoflavones increase insulin secretion and prevent the development of diabetic cataracts in streptozotocin-induced diabetic rats. *Nutrition Research*, 28(7), 464–471. <https://doi.org/10.1016/j.nutres.2008.03.009>
- Mendes, E. M., Irie, M. S., Rabelo, G. D., Borges, J. S., Dechichi, P., Diniz, R. S., & Soares, P. B. F. (2020). Effects of ionizing radiation on woven bone: Influence on the osteocyte lacunar network, collagen maturation, and microarchitecture. *Clinical Oral Investigations*, 24(8), 2763–2771. <https://doi.org/10.1007/s00784-019-03138-x>
- Napoli, N., Chandran, M., Pierroz, D. D., Abrahamsen, B., Schwartz, A. V., Ferrari, S. L., & IOF Bone and Diabetes Working Group. (2017). Mechanisms of diabetes mellitus-induced bone fragility. *Nature Reviews. Endocrinology*, 13(4), 208–219. <https://doi.org/10.1038/nrendo.2016.153>
- Nyman, J. S., Even, J. L., Jo, C. H., Herbert, E. G., Murry, M. R., Cockrell, G. E., Wahl, E. C., Bunn, R. C., Lumpkin, C. K., Jr., Fowlkes, J. L., & Thrailkill, K. M. (2011). Increasing duration of type 1 diabetes perturbs the strength-structure relationship and increases brittleness of bone. *Bone*, 48(4), 733–740. <https://doi.org/10.1016/j.bone.2010.12.016>
- Okubo, Y., Bessho, K., Fujimura, K., Kusumoto, K., Ogawa, Y., & Izuka, T. (2001). Effect of hyperbaric oxygenation on bone induced by recombinant human bone morphogenetic protein-2. *The British Journal of Oral & Maxillofacial Surgery*, 39(2), 91–95. <https://doi.org/10.1054/bjom.2000.0550>
- Palermo, A., D'Onofrio, L., Buzzetti, R., Manfrini, S., & Napoli, N. (2017). Pathophysiology of bone fragility in patients with diabetes. *Calcified Tissue International*, 100(2), 122–132. <https://doi.org/10.1007/s00223-016-0226-3>
- Prabowo, S., Nataatmadja, M., Hadi, J., Dikman, I., Handajani, F., Tehupuring, S., Soetarso, I., Suryokusumo, M., Aulani, A., Herawati, A., & West, M. (2014). Hyperbaric oxygen treatment in a diabetic rat model is associated with a decrease in blood glucose, regression of organ damage and improvement in wound healing. *Health*, 06, 1950–1958. <https://doi.org/10.4236/health.2014.615228>
- Rajagopalan, G., Kudva, Y. C., & David, C. S. (2012). Is HOT a cool treatment for type 1 diabetes? *Diabetes*, 61(7), 1664–1666. <https://doi.org/10.2337/db12-0527>
- Reyes-Fernandez, P. C., Periou, B., Decrouy, X., Relaix, F., & Authier, F. J. (2019). Automated image-analysis method for the quantification of fiber morphometry and fiber type population in human skeletal muscle. *Skeletal Muscle*, 9(1), 15. <https://doi.org/10.1186/s13395-019-0200-7>
- Rocha, F. S., Limirio, P. H., Zanetta-Barbosa, D., Batista, J. D., & Dechichi, P. (2016). The effects of ionizing radiation on the growth plate in rat tibiae. *Microscopy Research and Technique*, 79(12), 1147–1151. <https://doi.org/10.1002/jemt.22769>
- Schindelin, J., Rueden, C. T., Hiner, M. C., & Eliceiri, K. W. (2015). The ImageJ ecosystem: An open platform for biomedical image analysis. *Molecular Reproduction and Development*, 82(7–8), 518–529. <https://doi.org/10.1002/mrd.22489>
- Silva, A., Martins, S., Neves, L., de Faria, P., Tosta, T., & Zanchetta do Nascimento, M. (2019). Automated nuclei segmentation in dysplastic histopathological oral tissues using deep neural networks. In *Progress in pattern recognition, image analysis, computer vision, and applications* (pp. 365–374), Barbosa.
- Soares, P. B. F., Soares, C. J., Limirio, P., de Jesus, R. N. R., Dechichi, P., Spin-Neto, R., & Zanetta-Barbosa, D. (2019). Effect of ionizing radiation after-therapy interval on bone: Histomorphometric and biomechanical characteristics. *Clinical Oral Investigations*, 23(6), 2785–2793. <https://doi.org/10.1007/s00784-018-2724-3>
- Steiner, D. F., MacDonald, R., Liu, Y., Truszkowski, P., Hipp, J. D., Gammage, C., Thng, F., Peng, L., & Stumpe, M. C. (2018). Impact of deep learning assistance on the histopathologic review of lymph nodes for metastatic breast cancer. *The American Journal of Surgical Pathology*, 42(12), 1636–1646. <https://doi.org/10.1097/PAS.0000000000001151>
- Tammaing, G. G., Paulitsch-Fuchs, A. H., Jansen, G. J., & Euverink, G. W. (2016). Different binarization processes validated against manual counts of fluorescent bacterial cells. *Journal of Microbiological Methods*, 128, 118–124. <https://doi.org/10.1016/j.mimet.2016.07.003>
- Wang, S., Yang, D. M., Rong, R., Zhan, X., & Xiao, G. (2019). Pathology image analysis using segmentation deep learning algorithms. *The American Journal of Pathology*, 189(9), 1686–1698. <https://doi.org/10.1016/j.ajpath.2019.05.007>
- Wu, D., Malda, J., Crawford, R., & Xiao, Y. (2007). Effects of hyperbaric oxygen on proliferation and differentiation of osteoblasts from human alveolar bone. *Connective Tissue Research*, 48(4), 206–213. <https://doi.org/10.1080/03008200701458749>

SUPPORTING INFORMATION

Additional supporting information can be found online in the Supporting Information section at the end of this article.

How to cite this article: Linhares, C. R. B., Rabelo, G. D., Limirio, P. H. J. O., Venâncio, J. F., Ribeiro Silva, I. G., & Dechichi, P. (2022). Automated bone healing evaluation: New approach to histomorphometric analysis. *Microscopy Research and Technique*, 85(10), 3339–3346. <https://doi.org/10.1002/jemt.24188>

2.2 - Capítulo 2

Artigo a ser enviado para publicação no periódico Current Diabetes Reviews

(<https://benthamscience.com/public/journals/current-diabetes-reviews>)

Effect of hyperbaric oxygenation and insulin therapy on bone characteristics and mechanical properties in rats with type I diabetes mellitus

Linhares CRB¹, Limirio PHJO¹, Venâncio JF¹, Soares PBF¹, Dechichi P²

¹Dentistry Department, Federal University of Uberlândia, Bairro Umuarama, Uberlândia, Minas Gerais, Brazil, 38.405-320.

²Department of Cell Biology, Histology and Embryology, Biomedical Science Institute, Federal University of Uberlândia, Bairro Umuarama, Uberlândia, Minas Gerais, Brazil, 38.400-902.

***Corresponding author:** Paula Dechichi

Professor - Department of Cell Biology, Histology and Embryology Biomedical Science Institute, Federal University of Uberlândia.

Bairro Umuarama. Uberlândia – Minas Gerais – Brazil, 38.405-318.

Phone (fax): +55 (34) 32258481

Email: pauladechichi@ufu.br

Abstract

The aim of the study was to evaluate the effect of hyperbaric oxygenation (HO) and insulin therapy (IT) on microarchitecture, chemical composition and mechanical properties in tibiae of rats with type I Diabetes Mellitus (T1DM). Forty-eight rats were divided into 6 groups (n = 8): normoglycemic (N); normoglycemic + HO (NH); diabetic (D); diabetic + HO (DH); diabetic + insulin (DI); diabetic + insulin + HO (DIH). T1DM was induced by intravenous injection of streptozotocin (50mg/Kg). The DI and DIH groups received 4UI of NPH insulin/day. Thirty days after induction, NH, DH and DIH were subjected to hyperbaric oxygenation daily for 7 days and, 7 days after, the animals were euthanized, the tibiae removed and stored at -20°C. Subsequently, the tibiae were thawed and subjected to analysis: macroscopic, computed microtomography (micro-CT), three-point flexural test and infrared spectroscopy with Fourier transform (FTIR). In the results, D group showed length, cortical thickness, bone volume, anisotropy and collagen maturity lower than N and DI; and DIH showed higher macroscopic values than DH and DI. The fractal dimension was smaller in N compared to D and DI. Collagen maturity was higher in DIH, DH and NH compared to DI, D and N. In the ratio of organic/mineral matrices, D was lower than N. Maximum strength and stiffness were higher in N and NH compared to D and DH. It is concluded that type I Diabetes Mellitus compromised growth, microarchitecture, matrix composition and bone mechanical properties. Moreover, insulin therapy and hyperbaric oxygenation reduced the negative effects of type I Diabetes Mellitus.

Keywords: Diabetes Mellitus type 1; Bone regeneration; Hyperbaric Oxygenation; Insulin; Mechanical Phenomena; X-Ray Microtomography

Introduction

Type I diabetes mellitus (T1DM) is a metabolic disorder characterized by chronic hyperglycemia, that negatively alters microarchitecture and biomechanical properties of bone tissue (Ay et al. 2020; Limirio et al., 2024). In addition, T1DM compromise bone healing, increased fracture risk (Bai et al., 2020; Starup-Linde et al., 2016), and is related to higher rates of complications during surgery procedures (Martin et al., 2016). Studies suggest that bone impairment is due to the excess of advanced glycation end products (AGEs) in blood and its incorporation in the bone tissue (Yang et al., 2015). The accumulation of AGEs in the bone interferes in matrix quality and differentiation and function of bone cells (Yang et al., 2015).

Currently, insulin therapy is the treatment of choice for patients with DM1. This use is able to reduce blood glucose levels and allow it to be controlled. Recent studies show that patients with T1DM with controlled glycemia are significantly less affected by deleterious effects on bone biomechanical and microarchitecture tissue (Limirio et al., 2024), and mineral density rates (Susuki et al., 2022).

New therapies have been investigated and proposed to improve the bone repair process, especially in unfavorable conditions, such as diabetes. Hyperbaric oxygenation therapy (HO) has gained recognition for its potential to enhance bone repair (Dias et al., 2018), improved microcirculation (Mathieu et al., 2006), reduction of inflammation (Benson et al., 2003), and antibacterial effects (Mathieu et al., 2006). It consists of pure oxygen supply (100%) in a pressurized environment at a level above the atmospheric pressure, normally two to three more atmospheres.

Studies have reported that HO increases the amount of oxygen in blood and promotes angiogenesis in injured tissues, increasing the amount of oxygen and nutrients in the injured site (De Wolde et al., 2021; Jan et al., 2009), accelerating the repair process in soft (Izumino et al., 2020; Kalani et al., 2002) and mineralized tissues (Rocha et al. 2015; Dias et al. 2018). In the bone tissue, HO showed improvement in bone mechanical properties, increasing the strength and rigidity of the femur in T1DM animals (Limirio et al. 2018). Other studies demonstrate that HO, in healthy mice, increases the rate of bone mineral apposition and positively interferes with bone callus resorption and fracture

consolidation, accelerating the bone remodeling process in this situation (Kawada et al., 2013).

The specific effects of hyperbaric oxygen therapy and insulin therapy on the bones of patients with T1DM are not completely understood. The present study contributes to the understanding how these therapies interfere with bone characteristics and mechanical properties.

The objective of this study was to evaluate the effect of hyperbaric oxygenation (HO) and insulin therapy (IT) on microarchitecture, chemical composition and mechanical properties in tibiae of rats with type I Diabetes Mellitus (T1DM). The study hypothesis is that the association of hyperbaric oxygen therapy and insulin therapy positively affect microarchitecture, matrix composition, and bone mechanical properties in rats with T1DM. Thus, these interventions together could have the potential to eliminate the consequences of DM and make its bone structure similar to that of normoglycemic rats.

Material and methods

Experimental procedure

Forty-eight male Wistar rats (*Rattus norvegicus*) weighing 240 ± 20 g (8 weeks of age) were housed in standard conditions (12-hour light/dark cycle, temperature of $22 \pm 2^\circ\text{C}$ and relative humidity of 50–60%), with food (composition: humidity, crude protein, ethereal extract, mineral, crude fiber, calcium and phosphorus) and water *ad libitum*. After one week of acclimatization, the animals were randomly assigned and equally distributed into the following six groups (n=8): normoglycemic (N); normoglycemic + HO (NH); diabetic (D) and diabetic + HO (DH), diabetic + insulin (DI); and diabetic + insulin + HO (DIH). All animals were euthanized 44 days after diabetes induction.

All experimental protocols with animals were approved by the Committee on the Ethics of Animal Use and Care of the Federal University of Uberlândia (permit number 026/14). All procedures were carried out in strict accordance with the recommendations

in the Guide for the National Institutes of Health guide for the care and use of Laboratory animals (NIH Publications No. 8023, revised 1978).

Type 1 Diabetes Mellitus Induction (T1DM)

Type 1 Diabetes Mellitus Induction (T1DM) induction, follow-up evaluation, and glycemic assessment were performed as described by Limirio et al. (2018), the only change made was in the induction dosage (50 mg/kg). At time intervals of 2, 30, 37 and 44 days after diabetes induction, blood glucose was measured using a glucometer (Accu Check Active, Roche, Jaguaré, SP, Brazil). Animals that maintained blood glucose levels higher than 200 mg/dL were considered diabetic. During the experimental period, 4UI insulin was administered daily in the DI and DIH group (1UI at 7 am and 3 UI at 7 pm).

The Hyperbaric Oxygen therapy (HO) sessions started 30 days after induced T1DM and were performed as described by Rocha et al. (2015). The HO sessions were daily, in a cylindrical pressure chamber (Ecobar 400, Ecotec Equipamentos e Sistemas Ltda®, Mogi das Cruzes, SP, Brazil) at 2.5 ATA, in 90-minute sessions, totaling 7 sessions. The animals were euthanized after 7 days of HO completion. Both tibiae were removed by disarticulation and immediately placed in gauze impregnated with physiological saline solution and then kept frozen in a freezer (-20°C) (Limirio et al., 2018).

Macroscopic measurements

The tibia was measured using a pachymeter (Western, São Paulo, SP, Brazil). The unit of measurement used was millimeters. The measured parameters were proximal-distal length (PD), anteroposterior thickness (AP), lateral medial thickness (LM), anteroposterior proximal epiphysis (AP-D), lateral medial proximal epiphysis (LM-D), anteroposterior distal epiphysis (AP-P), distal lateral-medial epiphysis (LM-P) (Rocha et al., 2016).

Micro-CT

The tibia was scanned using computed micro tomography (μ CT-SkyScan 1272, Bruker, Kontich, Belgium), with a nominal isotropic voxel size of $8\mu\text{m}$ (X-ray source of 90 kVp, 111 μA). The reconstruction was done in 3D using the nRecon software (version 1.6.10.1, SkyScan, Bruker, Belgium), smoothing 1 and ring artifact correction. After that, they were analyzed in the CTAn software (version 1.14.4.1, SkyScan, Bruker, Belgium), using a threshold (higher than 255 and lower 65). The parameters used to analyze were: BS / BV (Specific bone surface [$\text{mm}^2 / \text{mm}^3$] - Ratio of the segmented bone surface to the segmented bone volume); Ct.Th (cortical thickness); DA (degree of anisotropy), FD (fractal dimension); Po.tot (total porosity).

Three-point flexural test

The tibia was analyzed in a three-point bending test until failure, using universal-testing machine (EMIC DL 2000, EMIC Equipamentos e Sistemas de Ensaio Ltda, São José dos Pinhais, Brazil). The specimen was placed horizontally on the two holding fixtures (16 mm) in the machine, the upper device load was applied in middle of the diaphysis at a loading rate of 1.0 mm/min. Load, displacement data were recorded, and subsequently, load vs. Displacement curves were plotted. Evaluations were derived from data with maximum strength (N), energy to- failure (mJ) and stiffness values (N/mm) and calculated as the slope of the initial linear uploading portion of the curves (Soares et al., 2019; Limirio et al., 2024).

Fourier Transform Infrared Spectroscopy (ATR-FTIR)

The tibia fractured after the mechanical test were maintained in phosphate buffered saline until the attenuated total reflectance Fourier transform infrared spectroscopy (ATR-FTIR) analysis. After the three-point bending test, it were obtained three fragments measuring 2x2 mm, with 2 mm thick from tibia and the ATR-FTIR of the tibia was performed as described by Limirio et al. (2018). The ATR-FTIR spectrums were further analyzed by calculating the following parameters: Amide I band (AI); Crystallinity Index (CI); Matrix-to-mineral ratio: Amide I + II/Hydroxyapatite (HA) (M:MI) and Amide III + Collagen/HA (M:MIII).

Statistical analysis

Statistical analysis was performed using statistical software Sigma Plot 13.1® (Systat Software Inc, San Jose, CA, USA). The results obtained were submitted to the Kolmogorov-Smirnov normality test and subsequently to the Two-Way ANOVA followed by the Tukey test. Results are presented as mean \pm standard deviation (SD). Differences were considered statistically significant when $\alpha < 0.05$.

Results

The success rate of diabetes induction in animals was 95% and mortality was less than 10%. Before induction, the mean glycemic levels of the animals were measured at 102.85 mg/dL. The mean glucose levels in different time measures for all groups are shown in Table 1 and Figure 1.

Table 1: Mean and standard deviation of Glucose level values at experimental times in the different groups

Glucose level (mg/dl)/groups	N	NH	D	DH	DI	DIH
Day 2	102.55 \pm 12.68	103.15 \pm 6.50	559.40 \pm 65.69	550.60 \pm 74.02	600 \pm 39.00	516.80 \pm 75.88
Day 30	124.60 \pm 35.39	106.40 \pm 17.69	594.20 \pm 8.14	600 \pm 22.00	206.20 \pm 157.20	205.80 \pm 126.04
Day 37	109.60 \pm 27.97	105.60 \pm 6.50	582.33 \pm 30.60	423.75 \pm 201.35	196 \pm 20917	181 \pm 106.73
Day 44	104.00 \pm 17.79	85.80 \pm 10.14	584.33 \pm 27.14	360 \pm 107.33	203.20 \pm 73.95	176 \pm 73.20
Total mean	112.73 \pm 8.84	99.27 \pm 6.50	586.96 \pm 12.09	461.25 \pm 83.52	289.20 \pm 68.21	187.60 \pm 13.66

Normoglycemic (N); Normoglycemic + HO (NH); Diabetics (D); Diabetics + HO (DH); Diabetics + Insulin (DI); Diabetics + HO + Insulin (DIH).

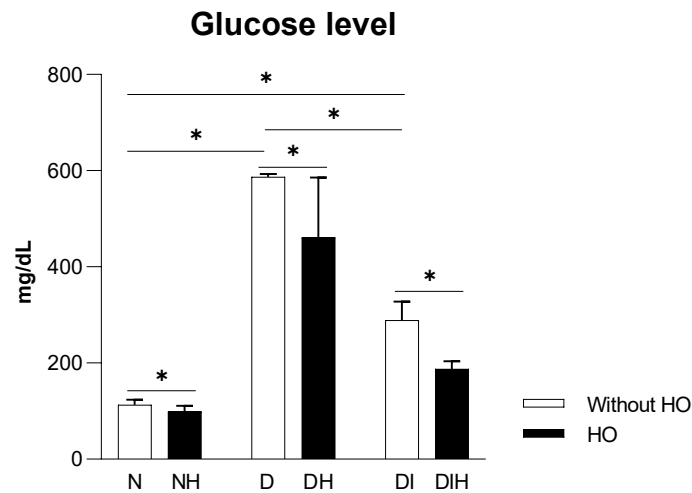


Figure 1: Glucose level in the different groups. * $p < 0,05$. Normoglycemic (N); Normoglycemic + HO (NH); Diabetics (D); Diabetics + HO (DH); Diabetics + Insulin (DI); Diabetics + HO + Insulin (DIH). The mean and SD values of glucose level analysis.

Macroscopic parameters

The results obtained from macroscopic analysis are shown in Table 2 and Figure 2. The normoglycemic group showed higher values compared with the diabetic group in the PD ($p < 0.05$) parameters. The values of the normoglycemic and diabetic + insulin groups were similar in all parameters with no significant difference between them ($p > 0.05$).

The macroscopic analysis demonstrated that rats from diabetic group (D) showed decreased Proximal-distal length (PD), Anteroposterior thickness (AP), Anteroposterior distal epiphysis (AP-P), Distal lateral-medial epiphysis (LM-P) and Lateral medial proximal epiphysis (LM-D) compared with normoglycemic group (N). The DIH group showed higher values compared with the D group in AP, AP-P e AP-D.

Table 2: Mean and standard deviation of Macroscopic parameters values in different groups

Parameters/Groups	N	NH	D	DH	DI	DIH
PD	39.90 ± 0.58Aa	39.59 ± 0.84Aa	37.57 ± 1.34Ba	37.88 ± 1.21Ba	38.94 ± 0.56Aa	39.41 ± 0.62Aa
AP	3.10 ± 0.19Aa	3.00 ± 0.12Aa	2.78 ± 0.26Ba	2.94 ± 0.22Ba	2.86 ± 0.14ABa	3.09 ± 0.15ABb
LM	2.51 ± 0.18Aa	2.50 ± 0.21Aa	2.33 ± 0.12Aa	2.45 ± 0.21Aa	2.36 ± 0.11Aa	2.49 ± 0.19Aa
AP-P	5.04 ± 0.22Aa	5.08 ± 0.30Aa	4.48 ± 0.30Ba	4.79 ± 0.36Bb	4.85 ± 0.27Aa	5.26 ± 0.36Ab
LM-P	4.30 ± 0.35Aa	3.98 ± 0.42Aa	3.66 ± 0.43Ba	3.66 ± 0.39Aa	4.01 ± 0.46Aa	3.97 ± 0.55Aa
AP-D	2.62 ± 0.23Aa	2.84 ± 0.25Ab	2.65 ± 0.16Aa	2.64 ± 0.23Aa	2.53 ± 0.18Aa	2.75 ± 0.15Ab
LM-D	2.27 ± 0.17Aa	2.27 ± 0.13Aa	2.08 ± 0.10Ba	2.17 ± 0.15Aa	2.11 ± 0.09Aa	2.21 ± 0.08Aa

In the rows, different capital letters indicate significant differences for diabetic factors (N and NH groups vs. D, DH, DI, DIH groups), and different lowercase letters indicate significant differences for hyperbaric oxygen therapy (N, D, DI vs. NH, DH, DIH) ($p < .05$). PD - Proximal-distal length, AP - Anteroposterior thickness, LM - Lateral medial thickness, AP-P - Anteroposterior distal epiphysis, LM-P - Distal lateral-medial epiphysis, AP-D - Anteroposterior proximal epiphysis, LM-D Lateral medial proximal epiphysis.

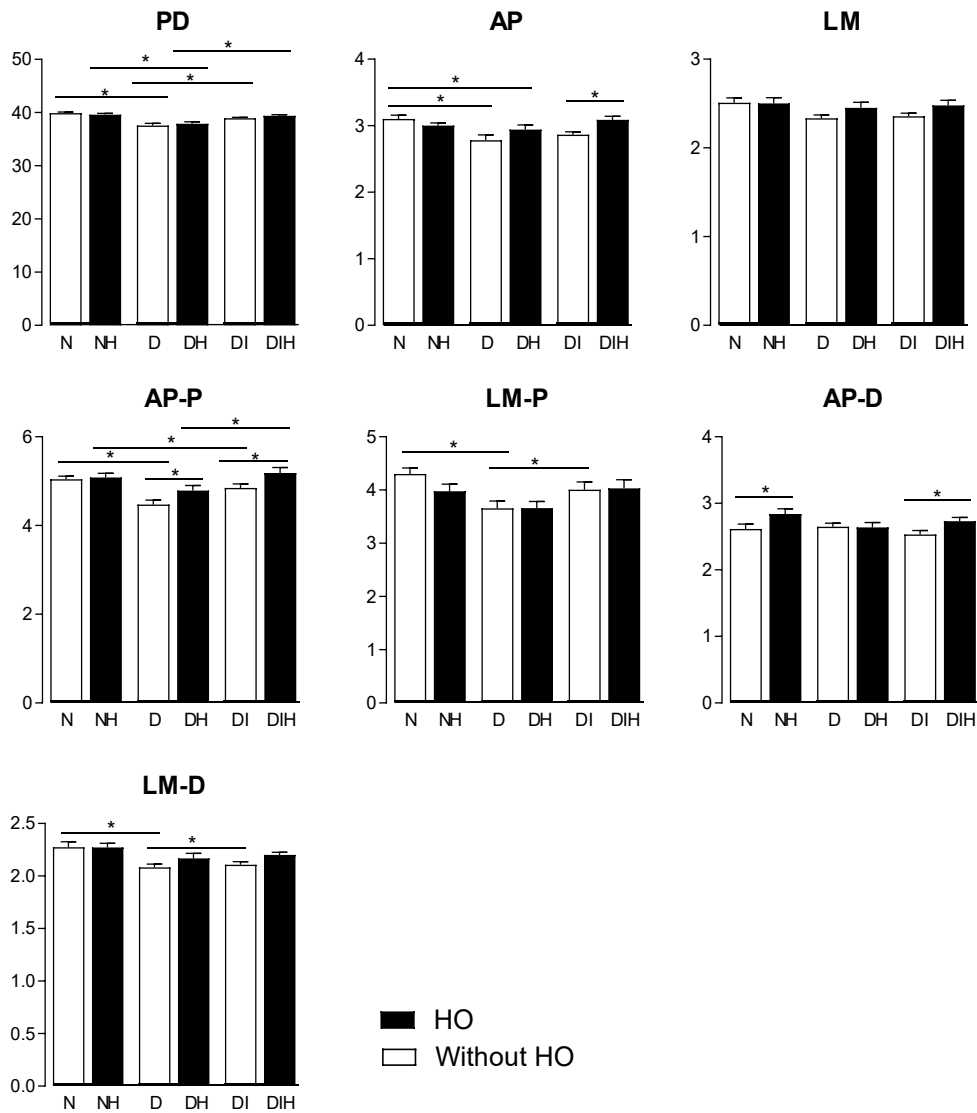


Figure 2: Macroscopic analysis of the parameters in the different groups.* $p < 0,05$. PD - Proximal-distal length, AP - Anteroposterior thickness, LM - Lateral medial thickness, AP-P - Anteroposterior distal epiphysis, LM-P - Distal lateral-medial epiphysis, AP-D - Anteroposterior proximal epiphysis, LM-D Lateral medial proximal epiphysis.

Micro-CT

The Micro-CT analysis results are shown in Table 3 and Figure 3. The N group showed higher values compared with the D group in the BS/BV, and Ct.Th. The values of BS/BV, DA, and Ct.Th of the N and DI groups were similar, with no significant difference between them ($p > 0.01$).

Table 3: Mean and standard deviation of Microcomputed tomography (MicroCT) analysis values in different groups

Parameters/Groups	N	NH	D	DH	DI	DIH
BS/BV	35.46 ± 0.77Aa	35.16 ± 1.25Aa	10.78 ± 0.56Ba	11.87 ± 0.83Aa	34.86 ± 1.92Aa	35.02 ± 0.78Aa
FD	2.48 ± 0.01Aa	2.36 ± 0.01Aa	2.37 ± 0.02Ba	2.45 ± 0.01Aa	2.46 ± 0.02Ba	2.47 ± 0.03Aa
Po.To	0.30 ± 0.13Aa	0.78 ± 0.30Aa	0.26 ± 0.21Aa	0.23 ± 0.21Aa	0.26 ± 0.15Aa	0.35 ± 0.17Aa
DA	0.28 ± 0.01Aa	0.28 ± 0.01Aa	0.19 ± 0.02Ba	0.22 ± 0.01Aa	0.29 ± 0.01Aa	0.29 ± 0.01Aa
Ct.Th	0.54 ± 0.01Aa	0.53 ± 0.03Aa	0.44 ± 0.05Ba	0.44 ± 0.02Aa	0.52 ± 0.01Aa	0.55 ± 0.02Aa

In the rows, different capital letters indicate significant differences for diabetic factors (N and NH groups vs. D, DH, DI, DIH groups), and different lowercase letters indicate significant differences for hyperbaric oxygen therapy (N, D, DI vs. NH, DH, DIH) ($p < .05$). BS/BV (Specific bone surface [$\text{mm}^2 / \text{mm}^3$] - Ratio of the segmented bone surface to the segmented bone volume); FD (fractal dimension); Po.tot (total porosity); DA (degree of anisotropy); Ct.Th (cortical thickness).

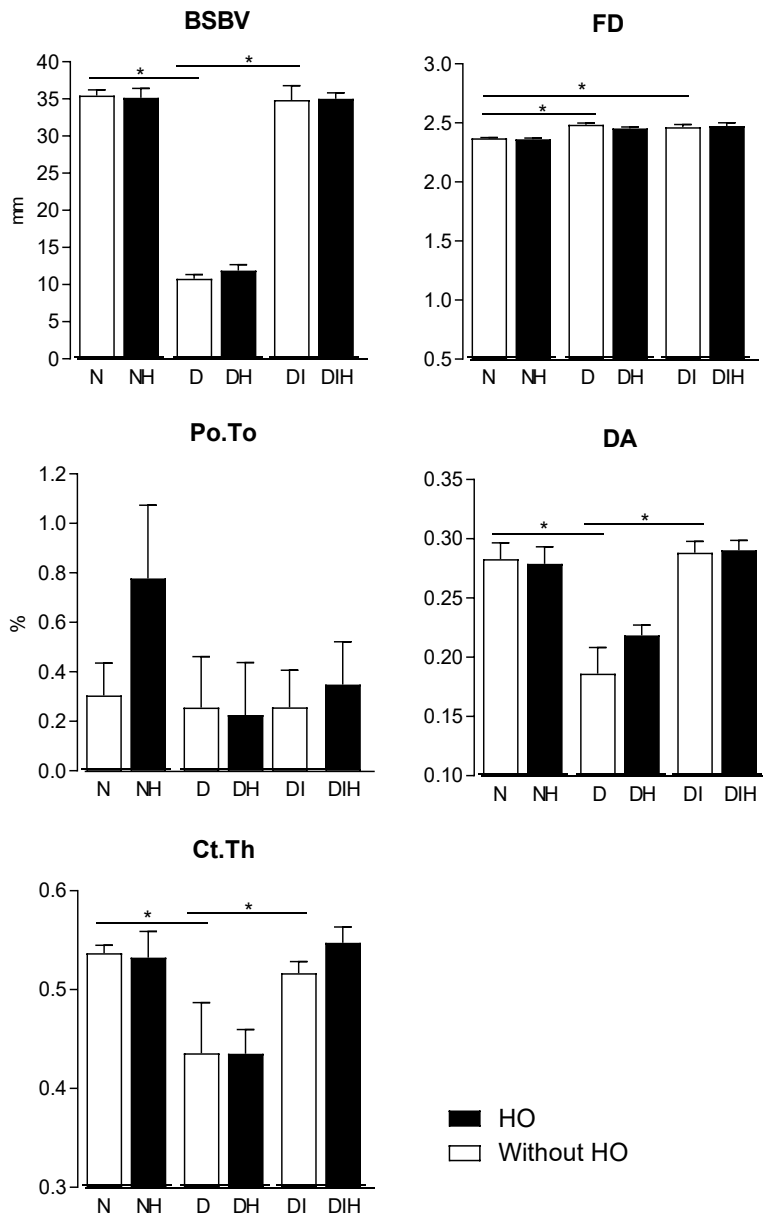


Figure 3: MicroCT analysis of the parameters in the different groups.* $p < 0,05$. BS/BV (Specific bone surface [$\text{mm}^2 / \text{mm}^3$] - Ratio of the segmented bone surface to the segmented bone volume); FD (fractal dimension); Po.tot (total porosity); DA (degree of anisotropy); Ct.Th (cortical thickness).

Three-point flexural test

The Three-point flexural test analysis results are shown in Table 4 and Figure 4. The N group showed higher values compared with the D group in the maximum strength. The values of maximum strength, energy, and stiffness of the N and DI groups were similar, with no significant difference between them ($p > 0.05$).

Table 4: Mean and standard deviation of Three-point flexural test analysis values in different groups

Parameters/Groups	N	NH	D	DH	DI	DIH
Maximum Strength	78.30 ± 7.59Aa	77.23 ± 8.61Aa	59.88 ± 5.74Ba	63.78 ± 8.04Ba	66.79 ± 6.61Ca	72.12 ± 7.32Ca
Energy	26.84 ± 3.50Aa	24.18 ± 6.25Aa	23.78 ± 5.36Aa	20.97 ± 5.29Aa	20.25 ± 5.80Ba	24.82 ± 2.44Ab
Stiffness	187.13 ± 30.05Aa	189.05 ± 22.99Aa	142.19 ± 31.23Ba	153.16 ± 33.38Ba	151.96 ± 31.32Ba	165.17 ± 19.97Aa

In the rows, different capital letters indicate significant differences for diabetic factors (N and NH groups vs. D, DH, DI, DIH groups), and different lowercase letters indicate significant differences for hyperbaric oxygen therapy (N, D, DI vs. NH, DH, DIH) ($p < .05$). N (normoglycemic); NH (normoglycemic + HO); D (diabetic); DH (diabetic + HO); DI (diabetic + insulin); DIH (diabetic + HO + insulin).

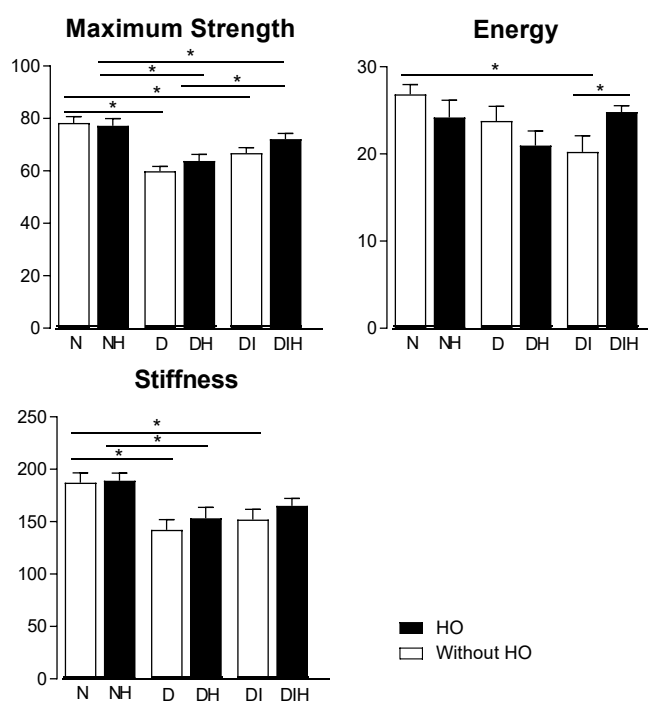


Figure 4: Three-point flexural test analysis of the parameters in the different groups.* $p < 0.05$.

Fourier Transform Infrared Spectroscopy (ATR-FTIR)

The Fourier Transform Infrared Spectroscopy analysis results are shown in Table 5 and Figure 5. The N group showed higher values compared with the D group in the

Amide I band, Crystallinity Index and Matrix-to-mineral ratio: Amide I + II/Hydroxyapatite (M:MI) ($p < 0.05$). The values of AI, IC and M:MI of the N and DI groups were similar, with no significant difference between them ($p > 0.05$).

The NH, DH, and DIH groups showed higher values compared with N, D and DI groups in the Amide I band and Crystallinity Index.

Table 5: The mean and SD values of Fourier Transform Infrared Spectroscopy analysis

Parameters/Groups	N	NH	D	DH	DI	DIH
AI	4.23 ± 0.83Aa	6.27 ± 0.90Ab	2.03 ± 0.49Ba	4.05 ± 0.66Bb	3.00 ± 0.72Ca	4.44 ± 0.71Cb
IC	3.43 ± 0.16Aa	3.68 ± 0.16Ab	2.81 ± 0.31Ba	3.42 ± 0.34Bb	3.42 ± 0.34Aa	3.69 ± 0.18Ab
M:MI	0.62 ± 0.02Aa	0.63 ± 0.04Aa	0.48 ± 0.02Ba	0.54 ± 0.03Aa	0.54 ± 0.03Aa	0.56 ± 0.01Aa
M:MIII	0.09 ± 0.01Aa	0.10 ± 0.01Aa	0.05 ± 0.01Ba	0.06 ± 0.01Bb	0.07 ± 0.01Aa	0.08 ± 0.01Aa

In the rows, different capital letters indicate significant differences for diabetic factors (N and NH groups vs. D, DH, DI, DIH groups), and different lowercase letters indicate significant differences for hyperbaric oxygen therapy (N, D, DI vs. NH, DH, DIH) ($p < .05$). AI - Amide I band; IC - Crystallinity Index; M:MI - Matrix-to-mineral ratio: Amide I + II/Hydroxyapatite; M:MIII - Amide III + Collagen/ Hydroxyapatite.

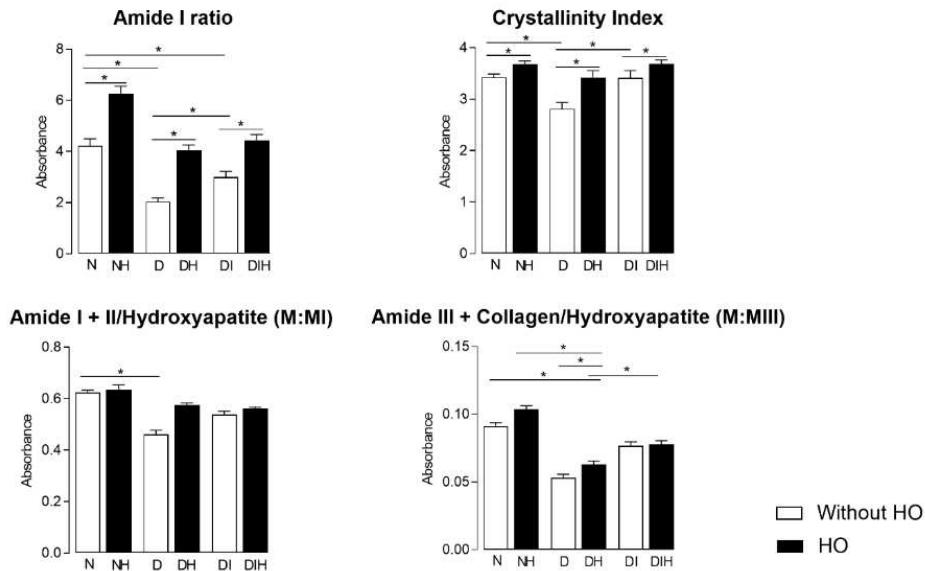


Figure 5: ATR-FTIR analysis of the parameters in the different groups.* $p < 0.05$. AI - Amide I band; IC - Crystallinity Index; M:MI - Matrix-to-mineral ratio: Amide I + II/Hydroxyapatite; M:MIII - Amide III + Collagen/ Hydroxyapatite.

Discussion

The present study hypothesized that decreased hyperglycemia with insulin therapy combined with hyperbaric oxygenation would eliminate the negative effects of T1DM on cortical bone microarchitecture, matrix composition and mechanical properties, restoring the parameters physiological conditions. In fact, our results showed that the association of insulin and hyperbaric oxygenation therapy minimized the deleterious effects of T1DM on bone microarchitecture, collagen maturation, crystalline HA content and mechanical properties of cortical bone.

The present study used an animal model to evaluate the structural changes of the cortical bone. T1DM induction was done through intravenous administration of streptozotocin, based on the toxic effect of this drug on pancreatic β cells, that induces a model of T1DM (Deeds et al., 2011) similar to that found in humans (Prabowo et al., 2014). The intravenous administration of STZ is currently the most stable and similar model to reproduce the disease, with a low rate of reversal and mortality (Dias et al., 2018; Deeds et al., 2011).

The bone affected by T1DM has different macroscopic parameters compared to the healthy bone. These parameters are essential to understanding how the disease affects the bone beyond the non-visible parameters. In this study the macroscopic parameters show that normoglycemic groups showed significantly higher values when compared to the diabetic group. This suggests that chronic hyperglycemia affects the process of endochondral ossification, which relies on the epiphyseal plate (Aeimlapa et al., 2014). In endochondral ossification, precursor cartilages are replaced by bone. Diabetes can interfere with this process in several ways: dysregulation of glucose metabolism (elevated blood glucose levels can affect cells involved in the ossification process, such as osteoblasts and chondroblasts, leading to compromised bone growth) (Wang et al., 2013); inhibition of collagen synthesis (diabetes can impair collagen synthesis, an essential protein for bone structure, resulting in weaker bones prone to deformities) (Saito et al., 2006); hormonal imbalance (diabetes can also affect hormone levels such as insulin and growth hormone, which play important roles in bone growth) (Napoli et al., 2019).

Furthermore, the insulin groups showed similar to the normoglycemic groups in macroscopic parameters, showing that glycemic control decreases the negative effects of T1DM, which confirms the hypothesis of the present study. This finding corroborates the Micro-CT, FTIR, and three-point flexural test results suggesting that T1DM decreased bone formation, leading to the loss of bone mass. Some studies have shown that this can occur because insulin deficiency impairs osteoblast function, while chronic hyperglycemia may inhibit osteoblast activity and promote osteoclast activity, resulting in decreased bone formation and increased bone resorption, respectively (Thraillkill et al., 2005). Additionally, chronic inflammation associated with T1DM and hormonal imbalance, along with potential nutritional deficiencies, also contribute to deteriorating bone health. These combined factors disrupt normal bone metabolism, leading to bone mass loss over time (Napoli et al., 2019).

The micro-CT methodology showed that BS/BV, DA and Ct.Th values in normoglycemic groups (N and NH) and the diabetic + insulin groups (DI and DIH) are significantly higher when compared with the diabetic group. The DI and DIH groups showed no significant difference in BS/BV, DA and Ct.Th compared to N and NH groups. This fact suggests the influence of chronic hyperglycemia can alter bone formation and reabsorption (remodeling processes) by increasing bone resorption or decreasing bone formation, leading to a reduction in bone density and changes in bone microarchitecture (Bao et al., 2023). Furthermore, hyperglycemia can negatively affect the differentiation and function of osteoblasts, the cells responsible for bone formation (Du et al., 2019; Wang et al., 2017). This can result in a reduction in bone formation and, consequently, in a decrease in the BS/BV parameter, indicating a smaller bone surface in relation to bone volume (Limirio et al., 2024).

The diabetic group showed more isotropic and heterogenous bone structure organization when compared with the normoglycemic group, presenting lower values of DA and higher values of FD. These findings suggest that T1DM causes significant alterations in bone channels alignment along the load directional axis (Silva et al., 2018) reducing the cortical complexity (Sellmeyer et al., 2016) and corroborating with bone fragility (Silva et al., 2018).

It was not found significant difference between M:MI and M:MIII ratio of diabetic + insulin group and the normoglycemic group. This this could be due to insulin therapy inhibit the collagen degradation (Saito et al. (2010). In addition, the diabetic group showed a lower M:MI and M:MIII ratio when compared with the normoglycemic group. This result suggests that the changes in collagen cross-linking, including increased AGEs harms the structure and function of collagen, compromising its ability to provide support and strength to the body's tissues (Saito et al., 2010).

The groups submitted hyperbaric oxygenation showed a higher value of amide I band, M:MI, M:III compared with the groups without hyperbaric oxygenation. This fact suggests the hyperbaric oxygenation can positively affect collagen in the bone of diabetics (Limirio et al., 2018). Studies indicate that HO promotes an increase in oxygen delivery to tissues, which can stimulate osteoblastic activity and the formation of new collagen. This can improve the quality of bone tissue, improving its structure (Saito et al., 2015).

The results of maximum biomechanical strength, energy, and stiffness values in diabetic groups, lower than the ones observed in normoglycemic groups could be due that chronic hyperglycemia leads to the accumulation of advanced glycation end products (AGEs), which negatively affect the strength and flexibility of collagen in bone, making bone tissue more fragile (Jiao et al., 2015; Saito et al., 2010). Furthermore, disturbances in the balance between bone formation and resorption, common in diabetics, can result in lower bone density and deterioration of bone microarchitecture.

Furthermore, the groups submitted to hyperbaric oxygenation reduced the blood glucose levels probable the effects of HO on partial regeneration pancreatic β -cells. Thus, being able to recover partially of insulin-producing function which reduces the glucose levels bringing diabetics closer to normoglycemic (Prabowo et al., 2014).

This study demonstrated that the combination of insulin therapy and hyperbaric oxygenation could reduce the negative alterations caused by T1DM. We noted significant improvements in key parameters such as amide I band, M:MI, M:III, which indicates changes in the composition and organization of collagen in relation to the bone mineral component. Furthermore, there are also improvements in the mechanical properties of parameters like strength, energy, and stiffness. These outcomes suggest a partial restoration of parameters to conditions closer to physiological, indicating a protective

effect of this therapeutic combination on bone health in the context of T1DM. The combination of insulin therapy and hyperbaric oxygenation offers a promising approach to preserving bone health in individuals with T1DM, mitigating the deleterious effects of this condition on bone microarchitecture, matrix composition, and mechanical properties.

Conclusion

The T1DM affects collagen maturation and mineral deposition reducing maximum strength, stiffness, and the capacity to absorb energy of the bone. Moreover, the association of Insulin therapy and hyperbaric oxygenation reduced the negative effects of T1DM.

References

1. Aeimlapa R, Wongdee K, Charoenphandhu N, Suntornsaratoon P, Krishnamra N. Premature chondrocyte apoptosis and compensatory upregulation of chondroregulatory protein expression in the growth plate of Goto-Kakizaki diabetic rats. *Biochemical and biophysical research communications*. 2014;452(3):395-401.
2. Ay B, Parolia K, Liddell RS, Qiu Y, Grasselli G, Cooper DML, et al. Hyperglycemia compromises Rat Cortical Bone by Increasing Osteocyte Lacunar Density and Decreasing Vascular Canal Volume. *Commun Biol*. 2020;3(1):20.
3. Bao K, Jiao Y, Xing L, Zhang F, Tian F. The role of wnt signaling in diabetes-induced osteoporosis. *Diabetology & Metabolic Syndrome*. 2023;15(1):84.
4. Benson RM, Minter LM, Osborne BA, Granowitz EV. Hyperbaric oxygen inhibits stimulus-induced proinflammatory cytokine synthesis by human blood-derived monocyte-macrophages. *Clin Exp Immunol*. 2003;134(1):57-62.
5. De Wolde SD, Hulskes RH, Weenink RP, Hollmann MW, Van Hulst RA. The Effects of Hyperbaric Oxygenation on Oxidative Stress, Inflammation and Angiogenesis. *Biomolecules*. 2021;11(8).

6. Deeds MC, Anderson JM, Armstrong AS, Gastineau DA, Hiddinga HJ, Jahangir A, et al. Single dose streptozotocin-induced diabetes: considerations for study design in islet transplantation models. *Laboratory animals*. 2011;45(3):131-40.
7. Dias PC, Limirio P, Linhares CRB, Bergamini ML, Rocha FS, Morais RB, et al. Hyperbaric Oxygen therapy effects on bone regeneration in Type 1 diabetes mellitus in rats. *Connect Tissue Res*. 2018;59(6):574-80.
8. Du JH, Lin SX, Wu XL, Yang SM, Cao LY, Zheng A, et al. The Function of Wnt Ligands on Osteocyte and Bone Remodeling. *J Dent Res*. 2019;98(8):930-8.
9. Goldman RJ. Hyperbaric oxygen therapy for wound healing and limb salvage: a systematic review. *PM R*. 2009;1(5):471-89.
10. Izumino J, Kaku M, Yamamoto T, Yashima Y, Kagawa H, Ikeda K, et al. Effects of hyperbaric oxygen treatment on calvarial bone regeneration in young and adult mice. *Archives of oral biology*. 2020;117:104828.
11. Jan A, Sandor GK, Brkovic BB, Peel S, Evans AW, Clokie CM. Effect of hyperbaric oxygen on grafted and nongrafted calvarial critical-sized defects. *Oral Surg Oral Med Oral Pathol Oral Radiol Endod*. 2009;107(2):157-63.
12. Jiao H, Xiao E, Graves DT. Diabetes and Its Effect on Bone and Fracture Healing. *Current osteoporosis reports*. 2015;13(5):327-35.
13. Kawada S, Wada E, Matsuda R, Ishii N. Hyperbaric hyperoxia accelerates fracture healing in mice. *PLoS One*. 2013;8(8):e72603.
14. Limirio P, da Rocha Junior HA, Morais RB, Hiraki KRN, Balbi APC, Soares PBF, et al. Influence of hyperbaric oxygen on biomechanics and structural bone matrix in type 1 diabetes mellitus rats. *PLoS One*. 2018;13(2):e0191694.
15. Limirio P, De Oliveira Neto NF, Venâncio JF, Linhares C, Soares PBF, Dechichi P. Insulin Therapy on Bone Macroscopic, Microarchitecture, and Mechanical Properties of Tibia in Diabetic Rats. *Current diabetes reviews*. 2024.

16. Martin ET, Kaye KS, Knott C, Nguyen H, Santarossa M, Evans R, et al. Diabetes and Risk of Surgical Site Infection: A Systematic Review and Meta-analysis. *Infection control and hospital epidemiology*. 2016;37(1):88-99.
17. Mathieu D, Favory R, Collet F, Linke J-C, Wattel F. Physiologic Effects of Hyperbaric Oxygen on Hemodynamics and Microcirculation. 2006. p. 75-101.
18. Napoli N, Chandran M, Pierroz DD, Abrahamsen B, Schwartz AV, Ferrari SL, et al. Mechanisms of diabetes mellitus-induced bone fragility. *Nat Rev Endocrinol*. 2017;13(4):208-19.
19. Prabowo S, Nataatmadja M, Hadi J, Dikman I, Handajani F, Ejt S, et al. Hyperbaric Oxygen Treatment in a Diabetic Rat Model Is Associated with a Decrease in Blood Glucose, Regression of Organ Damage and Improvement in Wound Healing. *Health*. 2014;06:1950-8.
20. Rocha FS, Gomes Moura CC, Rocha Rodrigues DB, Zanetta-Barbosa D, Nakamura Hiraki KR, Dechichi P. Influence of hyperbaric oxygen on the initial stages of bone healing. *Oral Surg Oral Med Oral Pathol Oral Radiol*. 2015;120(5):581-7.
21. Rocha FS, Limirio PHJO, Zanetta-Barbosa D, Batista JD, Dechichi P. The effects of ionizing radiation on the growth plate in rat tibiae. 2016;79(12):1147-51.
22. Saito M, Fujii K, Mori Y, Marumo K. Role of collagen enzymatic and glycation induced cross-links as a determinant of bone quality in spontaneously diabetic WBN/Kob rats. *Osteoporos Int*. 2006;17(10):1514-23.
23. Saito M, Marumo K. Collagen cross-links as a determinant of bone quality: a possible explanation for bone fragility in aging, osteoporosis, and diabetes mellitus. *Osteoporos Int*. 2010;21(2):195-214.
24. Saito M, Marumo K. Effects of Collagen Crosslinking on Bone Material Properties in Health and Disease. *Calcif Tissue Int*. 2015;97(3):242-61.
25. Sellmeyer DE, Civitelli R, Hofbauer LC, Khosla S, Lecka-Czernik B, Schwartz AV. Skeletal Metabolism, Fracture Risk, and Fracture Outcomes in Type 1 and Type 2 Diabetes. *Diabetes*. 2016;65(7):1757-66.

26. Silva L, Figueira Venâncio J, Loures A, Lopes D, Dechichi P, Rabelo G. Efeito do Diabetes Mellitus tipo I na organização espacial das trabéculas ósseas: análise por meio do processo de esqueletonização. *HU Revista*. 2018;44:7.
27. Soares P, Soares C, Limirio P, Jesus R, Dechichi P, Spin-Neto R, et al. Effect of ionizing radiation after-therapy interval on bone: histomorphometric and biomechanical characteristics. *Clinical Oral Investigations*. 2019;23.
28. Starup-Linde J, Lykkeboe S, Gregersen S, Hauge E-M, Langdahl BL, Handberg A, et al. Bone Structure and Predictors of Fracture in Type 1 and Type 2 Diabetes. *The Journal of Clinical Endocrinology & Metabolism*. 2016;101(3):928-36.
29. Suzuki M, Urai S, Fukuoka H, Hirota Y, Yamamoto M, Okada Y, et al. Relation between the insulin lowering rate and changes in bone mineral density: Analysis among subtypes of type 1 diabetes mellitus. 2022;13(9):1585-95.
30. Thrailkill KM, Lumpkin CK, Jr., Bunn RC, Kemp SF, Fowlkes JL. Is insulin an anabolic agent in bone? Dissecting the diabetic bone for clues. *Am J Physiol Endocrinol Metab*. 2005;289(5):E735-45.
31. Wang J, Wang B, Li Y, Wang D, Lingling E, Bai Y, et al. High glucose inhibits osteogenic differentiation through the BMP signaling pathway in bone mesenchymal stem cells in mice. *EXCLI journal*. 2013;12:584-97.
32. Wang X, Liu L, Zhang W, Zhang J, Du X, Huang Q, et al. Serum metabolome biomarkers associate low-level environmental perfluorinated compound exposure with oxidative /nitrosative stress in humans. *Environ Pollut*. 2017;229:168-76.
33. Wijenayaka AR, Kogawa M, Lim HP, Bonewald LF, Findlay DM, Atkins GJ. Sclerostin stimulates osteocyte support of osteoclast activity by a RANKL-dependent pathway. *PLoS One*. 2011;6(10):e25900.
34. Yang X, Gandhi C, Rahman MDM, Appleford M, Sun L-W, Wang X. Age-Related Effects of Advanced Glycation End Products (Ages) in Bone Matrix on Osteoclastic Resorption. *Calcified Tissue International*. 2015;97(6):592-601.

2.3 - Capítulo 3

Artigo a ser enviado para publicação no periódico *Microscopy Research & Technique*

(<https://analyticalsciencejournals.onlinelibrary.wiley.com/journal/10970029>)

Bone regeneration is improved by hyperbaric oxygenation and insulin therapy association in type I diabetes rats

Linhares CRB¹, Limirio PHJO¹, Soares PBF¹, Dechichi P²

¹Dentistry Department, Federal University of Uberlândia, Bairro Umuarama, Uberlândia, Minas Gerais, Brazil, 38.405-320.

²Department of Cell Biology, Histology and Embryology, Biomedical Science Institute, Federal University of Uberlândia, Bairro Umuarama, Uberlândia, Minas Gerais, Brazil, 38.400-902.

***Corresponding author:** Paula Dechichi

Professor - Department of Cell Biology, Histology and Embryology Biomedical Science Institute, Federal University of Uberlândia.

Bairro Umuarama. Uberlândia – Minas Gerais – Brazil, 38.405-318.

Phone (fax): +55 (34) 32258481

Email: pauladechichi@ufu.br

Abstract

This study aimed to evaluate the effect of hyperbaric oxygenation (HO) and insulin therapy (IT) on bone regeneration in the femurs of rats with Type I Diabetes Mellitus (T1DM). Forty-eight rats were divided into 6 groups (n=8): Normoglycemic (N); Normoglycemic + HO (NH); Diabetics (D); Diabetics + HO (DH); Diabetics + Insulin (DI); Diabetics + HO + Insulin (DIH). T1DM was induced by intravenous injection of streptozotocin (50mg/Kg). The DI and DIH groups received 4UI of NPH insulin/day. Thirty days after induction, bone defects were performed in the femurs of all groups. Immediately after surgery, the NH, DH, and DIH groups were submitted to HO for 7 days. After this period, all animals were euthanized, the femurs removed, and fixed in 10% buffered formaldehyde. The femurs were analyzed by computed microtomography (micro-CT) considering: volume fraction (BV/TV) and bone surface (BS/BV); number (Tb.N), thickness (Tb.Th), separation (Tb.Sp) and connectivity (Conn.Dn) of trabeculae; fractal dimension (FD) and degree of anisotropy (DA). Then, the femurs was demineralized and processed to paraffin embedded. The bone matrix percentage was quantified in histological images. The results of the BV/TV and Tb.Th showed lower values group D than N and DI. In the BS/BV, group D showed a greater value than N and DI. In the FD, the N and NH groups showed higher values than D and DH, respectively. In Tb.N, Tb.Sp, Conn.Dn and DA there was no significant difference. In the histomorphometry, the groups D and DH showed lower percentage of the bone matrix when compared to the groups N, NH, DI, and DIH. No statistical difference was observed between groups N, NH, DI and DIH. It is concluded that T1DM compromised bone regeneration, and insulin therapy associated with HO reduced remarkably the bone deleterious effects of T1DM.

Keywords: Diabetes Mellitus; Bone regeneration; Hyperbaric Oxygenation

Introduction

Bone regeneration is a challenge in diabetic individuals, since the chronic hyperglycemia compromise angiogenesis and cells recruitment to the injury site, leads to delay in wound healing (Ay et al. 2020). This delay in the initial stages lead a cascading effect on bone repair processes. Osteoblast reduces the ability to produce the essential bone matrix components, that compromises the early stages of bone repair and may lead to suboptimal callus formation at the fracture site (Claes et al., 2011; Claes et al., 2012). Moreover, occurs formation of altered bone matrix composition caused by accumulation of advanced glycation end-products (AGEs) (Ay et al. 2020), and increased inflammation (Rubin, 2017; Vashishth, 2009). Persistent inflammation may lead to aberrant bone remodeling, affecting the strength and stability of the healed bone (Claes et al., 2012), and a higher risk of surgical complications (Martin et al., 2016).

Studies have suggested that Hyperbaric Oxygenation may stimulate osteogenesis, angiogenesis, and collagen production, essential for effective bone repair (Gajendrareddy et al., 2017; De Wolde et al., 2021). In the case of type I Diabetes Mellitus, impaired vascularization and reduced oxygen supply to bone tissues are common challenges. HO has the potential to counteract these issues by promoting the formation of new blood vessels and enhancing oxygen availability, thereby supporting the bone regeneration process. Improved vascularization ensures that essential nutrients and oxygen reach the site of bone repair, fostering a more robust and efficient healing process (Eldisoky et al., 2023). Furthermore, other studies have shown that HO can lower blood glucose in T1DM (Prabowo et al., 2014).

Hyperbaric oxygenation involves exposing patients to pure oxygen at increased atmospheric pressure. This results in a significant elevation of oxygen levels in the blood, promoting oxygen delivery to tissues, including the surgical site. In diabetics, compromised vascularization can limit oxygen supply to the healing bone. HO addresses this by enhancing oxygen diffusion, creating an oxygen-rich environment conducive to optimal bone repair (Jan et al., 2009; Izumino et al., 2020). In this context, hyperbaric oxygen therapy (HO) has been recognized for enhancing tissue healing by increasing oxygen delivery to compromised areas. In addition, HO stimulate angiogenesis (Mathieu

et al., 2006), reduce inflammation (Benson et al., 2003), increase collagen synthesis (Gajendrareddy et al., 2017), improving wound healing (Limirio et al. 2018; Dias et al., 2018).

The classic diabetes treatment is insulin therapy. Insulin, a hormone produced by the pancreas, plays a crucial role in glucose metabolism. Individuals with T1DM lack insulin, leading to elevated blood glucose levels. Apart from its role in glucose regulation, insulin has been recognized for its impact on bone health. Insulin receptors are present on osteoblasts and osteoclasts, indicating a direct influence on bone metabolism (Thraillkill et al., 2005). Furthermore, insulin has been shown to stimulate the production of growth factors like insulin-like growth factor 1 (IGF-1), which is essential for bone growth and repair (Thraillkill et al., 2005).

The combined use of hyperbaric oxygenation and insulin therapy may offer a synergistic approach to address bone regeneration in T1DM. Hyperbaric oxygenation provides the necessary oxygen support for cellular activities involved in bone healing, while insulin therapy targets the underlying metabolic imbalance associated with diabetes. The present study evaluated the potential synergistic effects of hyperbaric oxygenation and insulin therapy on bone regeneration in the femurs of rats with T1DM.

Material and methods

Experimental procedure

Forty-eight male Wistar rats (*Rattus norvegicus*) weighing 240 ± 10 g (8 weeks of age) were housed in standard conditions (12-hour light/dark cycle, temperature of $22 \pm 2^\circ\text{C}$ and relative humidity of 50–60%), with food (composition: humidity, crude protein, ethereal extract, mineral, crude fiber, calcium and phosphorus) and water ad libitum. After one week of acclimatization, the animals were randomly assigned and equally distributed into the following six groups (n=8): normoglycemic (N); normoglycemic + HO (NH); diabetic (D) and diabetic + HO (DH), diabetic + insulin (DI);

and diabetic + insulin + HO (DIH). All animals were euthanized 44 days after diabetes induction.

All experimental protocols with animals were approved by the Committee on the Ethics of Animal Use and Care of the Federal University of Uberlândia (permit number 026/14). All procedures were conducted in strict accordance with the recommendations in the Guide for the National Institutes of Health guide for the care and use of Laboratory animals (NIH Publications No. 8023, revised 1978).

The induction, monitoring, and glycemic evaluation for Type 1 Diabetes Mellitus (T1DM) followed the methodology outlined by Limirio et al. (2018), with the sole modification being the induction dosage adjusted to 50 mg/kg. Blood glucose levels were assessed at intervals of 2, 30, 37, and 44 days post-diabetes induction using a glucometer (Accu Check Active, Roche, Jaguaré, SP, Brazil). Animals maintaining blood glucose levels exceeding 200 mg/dL were classified as diabetic. It was administered 4UI insulin daily in the DI and DIH group (1UI at 7 am and 3 UI at 7 pm).

Clinical manifestations associated with diabetes, such as increased appetite (polyphagia), excessive thirst (polydipsia), and body weight, was measured in a quantitative analysis.

The Hyperbaric Oxygen therapy (HO) sessions started 30 days after induced T1DM and were performed as described by Rocha et al. (2015). The HO sessions were daily, in a cylindrical pressure chamber (Ecobar 400, Ecotec Equipamentos e Sistemas Ltda®, Mogi das Cruzes, SP, Brazil) at 2.5 ATA, in 90-minute sessions, with a total of seven sessions conducted.

The animals were euthanized after 44 days. Both femurs were removed by disarticulation and immediately placed in gauze impregnated with physiological saline solution and then kept frozen in a freezer (-20°C) (Limirio et al., 2018).

Micro-CT

The femurs underwent scanning to capture high-quality images, with a focus on selecting the bone defect area as the region of interest (ROI). Micro-CT scans were

conducted using a Sky-Scan 1272 scanner from Bruker in Kontich, Belgium, with the following parameters: 80 kV voltage, 125 μ A tube current, 1mm aluminum filter, 180° rotation, 0.6 rotation step, and 8 μ m resolution pixel size (**Figure 1**). The conversion of linear X-ray attenuation coefficients to volumetric tissue mineral densities was achieved through a calibration scan of the hydroxyapatite (HA) phantom. Image reconstruction was conducted using NRecon software (v.1.6.9.10, Bruker, Kontich, Belgium) and automatic processes were employed to distinguish and separate trabecular and cortical bone (CT Analyzer, v. 1.14.4.1+(64-bit), SkyScan, Bruker, Kontich, Belgium) (**Figure 2**) (**Figure 3**).

The parameters used to analyze the bone repair area were: Bone volume fraction (BV/TV); Trabecular Number (Tb.N [1/mm]); Trabecular separation (TB.Sp [mm]); Degree of anisotropy (DA); Bone surface fraction (BS/BV mm⁻¹); Trabecular thickness (TB.Th); Fractal dimension (FD); Connectivity density (Conn.Dn).

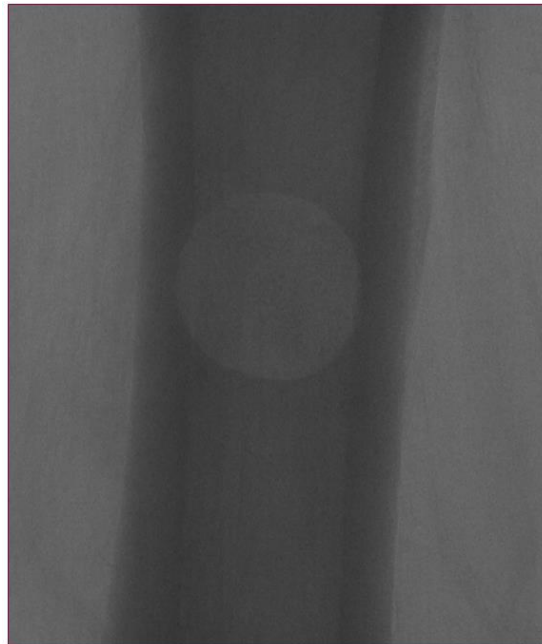


Figure 1: Pre-scan initial image (SKYSCAN 1272, Bruker, Belgium). Scanning carried out with a resolution of 08 μ m (80kvp, 125 μ A). Post-scanning, the 3D reconstruction area was delimited.

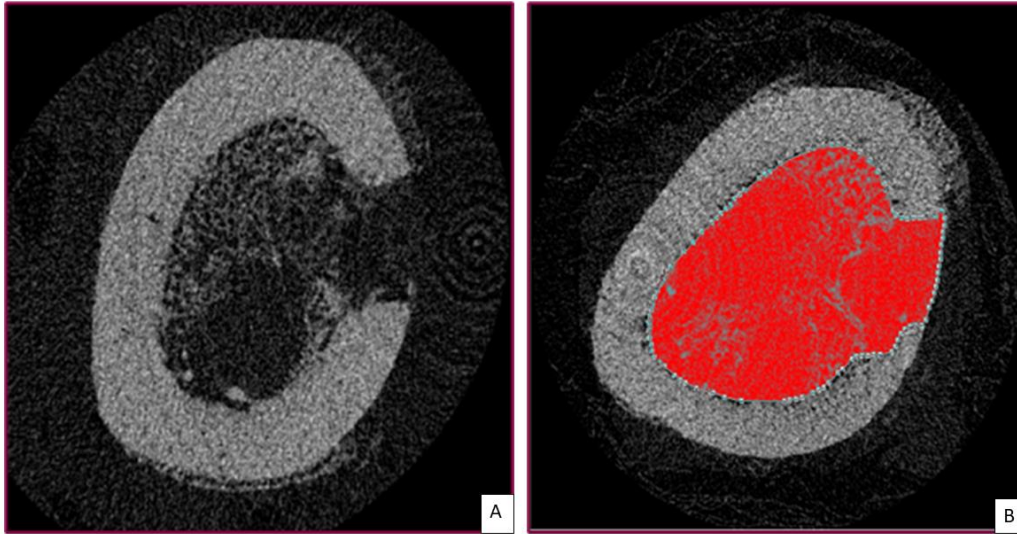


Figure 2: **A** - Transaxial section showing cortical bone and lesion area. **B** - Delimitation of the region of interest (ROI) containing the lesion area and spinal space.

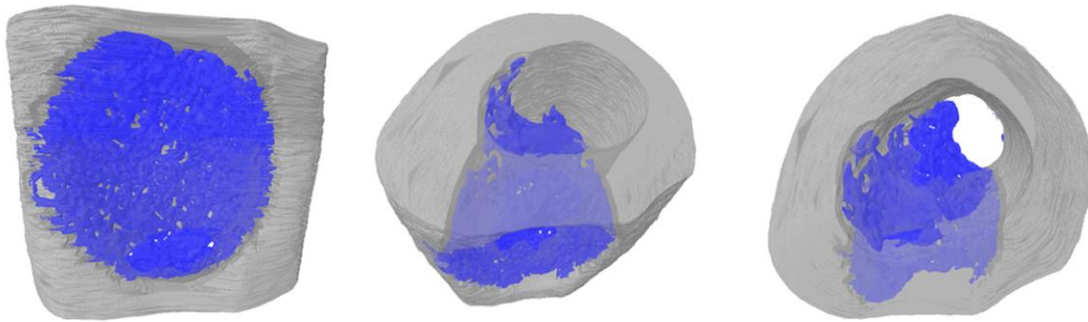


Figure 3: 3D MicroCT Reconstruction Model: This image displays a detailed three-dimensional model showcasing the bone lesion area.

Histomorphometric analysis

The histological processing (fixation, decalcification, inclusion, microtomy, and staining) followed the methodology outlined by Linhares et al. (2022). The quantification of the bone matrix employed the histological automated image analysis method as detailed in Linhares et al. (2022).

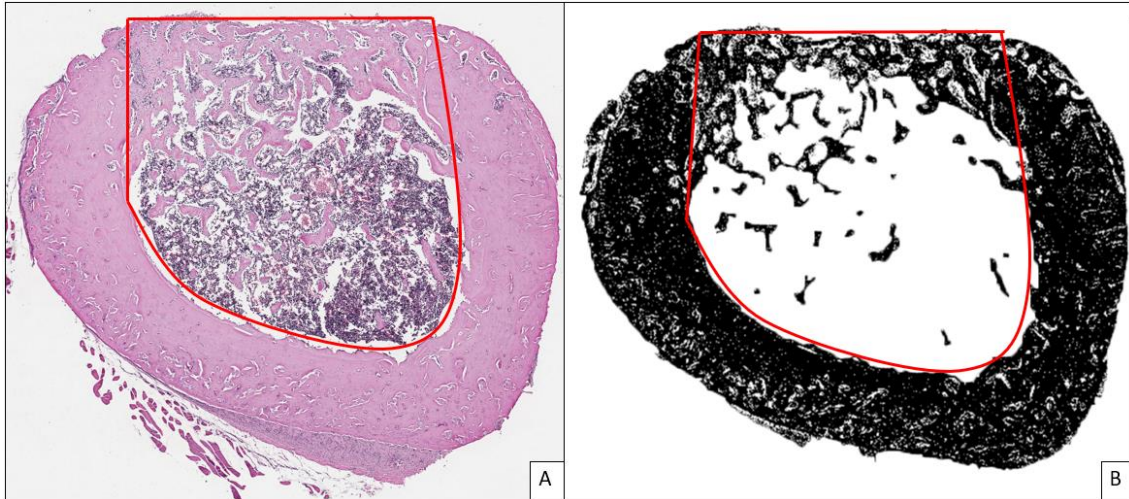


Figure 4: A - Histological image showing the region of the lesion (ROI). Hematoxylin and Eosin, 4X. B - Binary image showing the region of injury (ROI).

Statistical analysis

Statistical analysis was performed using statistical software Sigma Plot 13.1® (Systat Software Inc, San Jose, CA, USA). The results obtained were submitted to the Kolmogorov-Smirnov normality test and subsequently to the Two-Way ANOVA followed by the Tukey test. Results are presented as mean \pm standard deviation (SD). Differences were considered statistically significant when $\alpha < 0.05$.

Results

The success rate of diabetes induction in animals was 95% and mortality was less than 10%. Before induction, the glycemic levels of the animals were measured at 105 mg/dL. The mean glucose levels in different time measures for all groups are shown in Table 1 and Figure 5.

After induction, the diabetic group (D) and diabetic group + HO (DH) was increased feed consumption, water intake, and urinary excretion confirmed weight reduction, polyphagia, polydipsia, and polyuria. The mean of body weight, the water and food consumption values in different time measures for all groups are shown in Table 2.

Table 1: Glucose level values at experimental times in the different groups

Glucose level (mg/dl)/groups	N	NH	D	DH	DI	DIH
Day 2	108 ± 12.68	103.15 ± 6.50	495.25 ± 84.31	522 ± 55.83	503.20 ± 39.97	353.20 ± 140.44
Day 30	122 ± 25.21	95.40 ± 17.69	551 ± 65.79	529 ± 104.01	63.80 ± 24.22	77.80 ± 30.69
Day 37	113.56 ± 21.11	102.40 ± 6.50	542.67 ± 57	490 ± 52.49	111.80 ± 54.85	131.50 ± 106.73
Day 44	105.91 ± 16.71	87.60 ± 10.14	538 ± 27.62	464.14 ± 136.63	203.60 ± 69.71	124.33 ± 4.51
Total mean	113.82 ± 8.05	95.13 ± 7.40	543.89 ± 6.59	494.48 ± 32.81	126.40 ± 71.03	111.21 ± 29.16

Normoglycemic (N); Normoglycemic + HO (NH); Diabetics (D); Diabetics + HO (DH); Diabetics + Insulin (DI); Diabetics + HO + Insulin (DIH). The mean and SD values of glucose level analysis.

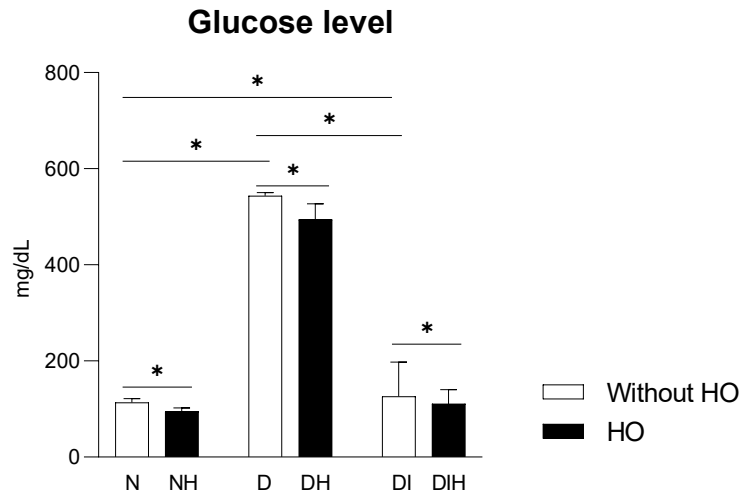


Figure 5: Glucose level in the different groups. * p<0,05. Normoglycemic (N); Normoglycemic + HO (NH); Diabetics (D); Diabetics + HO (DH); Diabetics + Insulin (DI); Diabetics + HO + Insulin (DIH). The mean and SD values of glucose level analysis.

Table 2: Mean and standard deviation of Parameters values in the different groups

Parameters/ groups	N	NH	D	DH	DI	DIH
Food consumption (grams)	154.33 ± 134	152 ± 72.47	174 ± 67.97	164.67 ± 37.60	117.67 ± 22.82	113.67 ± 23.87

Water consumption (mL)	302.17 ± 214.55	278.50 ± 159.70	645.83 ± 116.25	595 ± 108.49	259.17 ± 57.39	254.17 ± 86.86
Body weight (grams)	316.58 ± 43.92	317.49 ± 37.11	278.57 ± 25.06	293.31 ± 23.53	294.37 ± 36.82	317.76 ± 36.01

Normoglycemic (N); Normoglycemic + HO (NH); Diabetics (D); Diabetics + HO (DH); Diabetics + Insulin (DI); Diabetics + HO + Insulin (DIH). The mean and SD values of body weight analysis.

Micro-CT

Micro-CT analysis showed a higher values of bone volume fraction (BV/TV), trabecular thickness (TB.Th), bone surface fraction (BS/BV mm⁻¹), fractal dimension (FD) in the N, NH, DI and DIH groups than D and DH groups.

The Micro-CT analysis results are show in Table 3 and Figure 6.

Table 3: Mean and standard deviation MicroCT analysis values for different groups

Parameters/Groups	N	NH	D	DH	DI	DIH
BV/TV	25.7 ± 7.1Aa	27.9 ± 7.2Aa	13.5 ± 1.3Ba	17.4 ± 3.4Ba	26.8 ± 6.2Aa	26.3 ± 1.0Aa
Tb.N	5.9 ± 1.7Aa	6.7 ± 1.8Aa	4.2 ± 0.3 Aa	4.5 ± 1.0 Aa	6.3 ± 0.7 Aa	6.5 ± 0.6 Aa
TB.Sp	0.1 ± 0.0 Aa	0.1 ± 0.0 Aa	0.2 ± 0.0 Aa	0.2 ± 0.01 Aa	0.2 ± 0.1 Aa	0.3 ± 0.0 Aa
DA	0.4 ± 0.0 Aa	0.5 ± 0.03 Aa	0.4 ± 0.03 Aa	0.4 ± 0.1 Aa	0.4 ± 0.0 Aa	0.4 ± 0.0 Aa
BS/BV	101.0 ± 01.8Aa	103.5 ± 0.76Aa	32.8 ± 4.00Ba	58.7 ± 2.3Ba	91.2 ± 9.3 Aa	98.3 ± 0.17 Aa
Tb.Th	0.04 ± 0.00Aa	0.04 ± 0.00Aa	0.03 ± 0.00Ba	0.03 ± 0.01Ba	0.04 ± 0.01Aa	0.04 ± 0.0Aa
FD	2.6 ± 0.02Aa	2.6 ± 0.02Aa	2.4 ± 0.04Ba	2.5 ± 0.09Ba	2.5 ± 0.06ABa	2.5 ± 0.0ABa
Conn.Dn	0.2 ± 0.07 Aa	0.2 ± 0.06 Aa	0.2 ± 0.01 Aa	0.1 ± 0.03 Aa	0.2 ± 0.03 Aa	0.2 ± 0.0 Aa

In the rows, different capital letters indicate significant differences for diabetic factors (N and NH groups vs. D, DH, DI, DIH groups), and different lowercase letters indicate significant differences for hyperbaric oxygen therapy (N, D, DI vs. NH, DH, DIH) (p < .05). Bone volume fraction (BV/TV); Trabecular Number (Tb.N [1/mm]); Trabecular separation (TB.Sp [mm]); Degree of anisotropy (DA); Bone surface fraction (BS/BV mm⁻¹); Trabecular thickness (TB.Th); Fractal dimension (FD); Connectivity density (Conn.Dn).

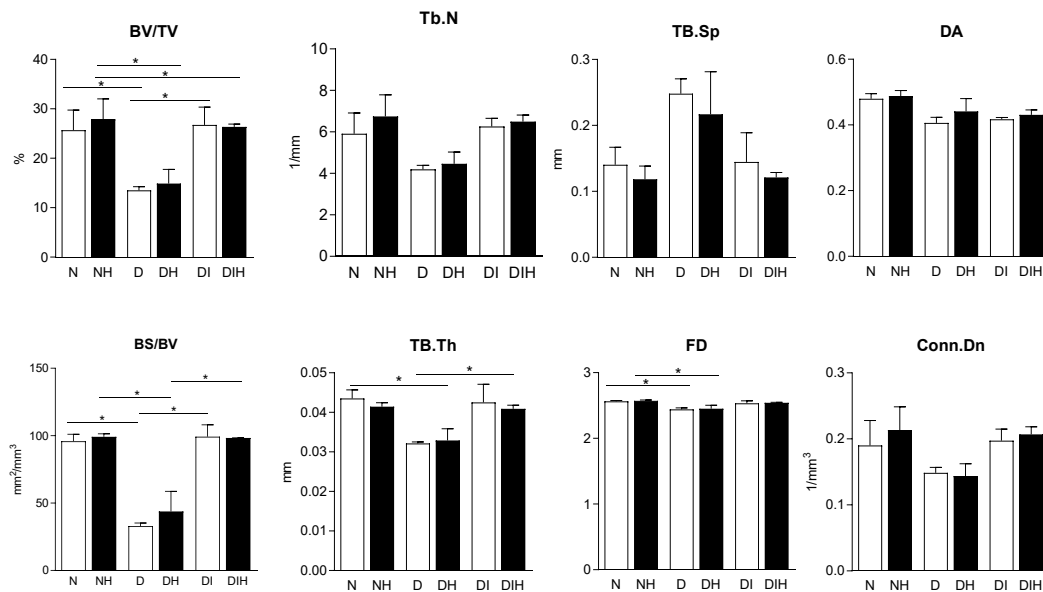


Figure 6: MicroCT analysis of the parameters in the different groups.* $p < 0.05$. Bone volume fraction (BV/TV); Trabecular Number (Tb.N [1/mm]); Trabecular separation (TB.Sp [mm]); Degree of anisotropy (DA); Bone surface fraction (BS/BV mm^{-2}); Trabecular thickness (TB.Th); Fractal dimension (FD); Connectivity density (Conn.Dn). The mean and SD values of histomorphometric analysis in the bone regeneration area.

Histological analysis

In the group N (Figure 7A; 7B), the histological analysis showed ROI partially filled with primary bone, many osteoblasts, and few osteoclasts.

The NH group (Figure 7C; 7D) also showed primary bone filling almost all of the ROI. The trabeculae were thicker compared to other groups, with many areas of osteoclastic activity. There were few red blood cells and many young osteoblasts associated with osteoid matrix. Bone regeneration in NH Group was at a more advanced stage compared with N Group.

Histological morphology in D (Figure 7E; 7F) and DH (Figure 7G; 7H), groups was similar to that of N Group, but in the diabetic were observed thinner trabecular with few osteoclasts. However, the diabetic group with HO (DH) showed increase in the bone regeneration process when compared with the diabetic group (D), and apparently similar to N group.

In DI (Figure 7I; 7J) and DIH (Figure 7K; 7L), groups were similar to N and NH they are very close to the condition of the normoglycemic presenting a discrete reduction trabecular with few osteoclasts.

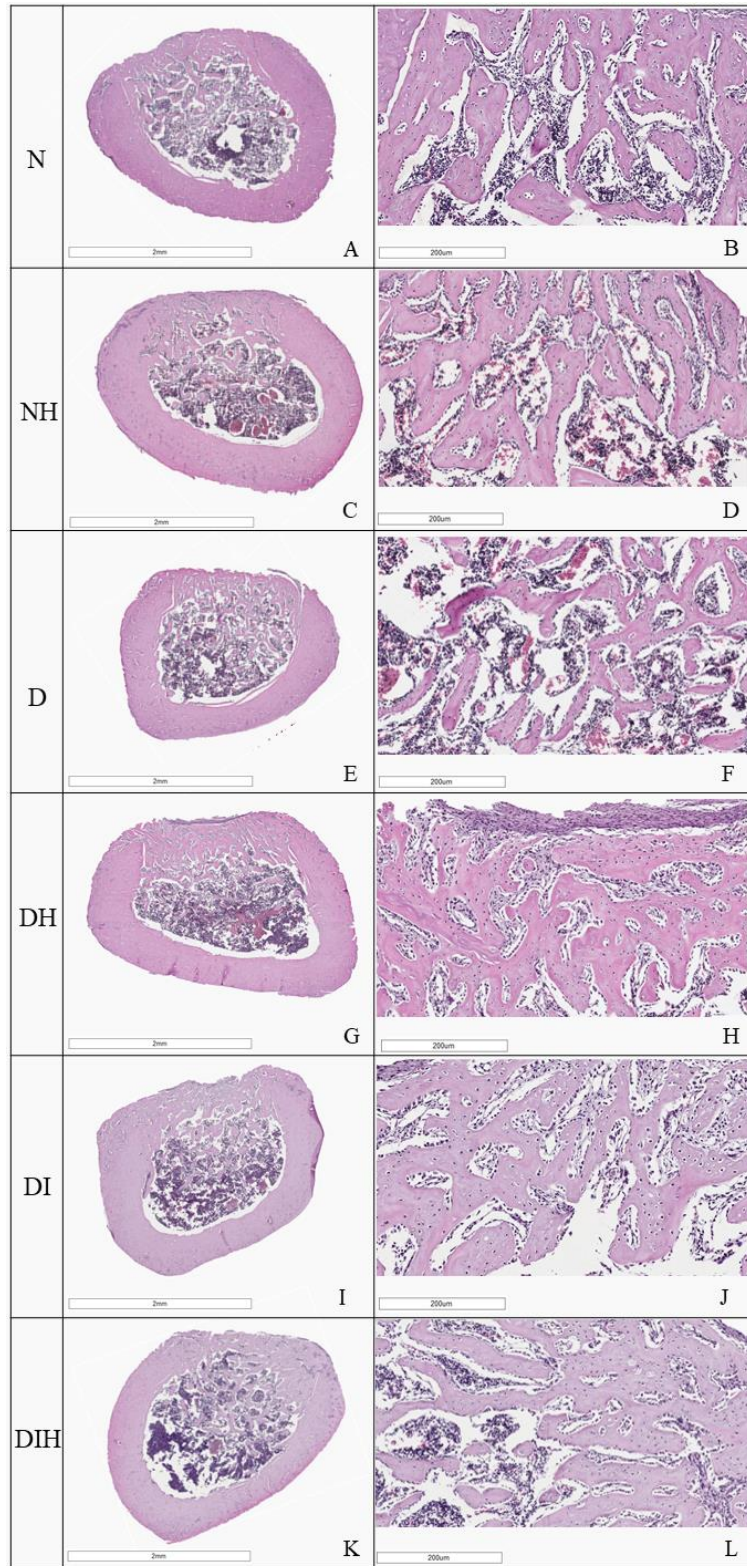


Figure 7: Histological images of femur cross-section. Hematoxylin and Eosin. Normoglycemic (N); Normoglycemic + HO (NH); Diabetics (D); Diabetics + HO (DH); Diabetics + Insulin (DI); Diabetics + HO + Insulin (DIH).

Histomorphometric analysis

The N (30.88 ± 1.40), NH (32.00 ± 1.40), DI (29.52 ± 1.25) and DIH (30.19 ± 1.43) groups showed a higher bone matrix values than D (27.79 ± 1.23) and DH (28.96 ± 2.22).

The Histomorphometric analysis results are show in Figure 8

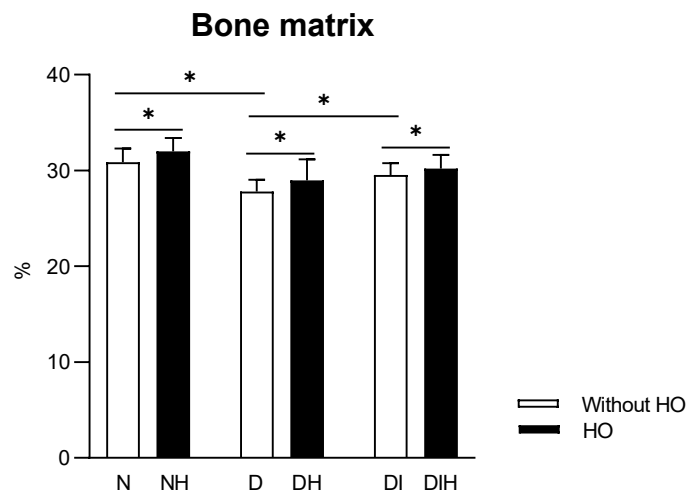


Figure 8: Histomorphometric results of histological image analysis in the different groups (* $p < 0.05$). Normoglycemic (N); Normoglycemic + HO (NH); Diabetics (D); Diabetics + HO (DH); Diabetics + Insulin (DI); Diabetics + HO + Insulin (DIH).

Discussion

Diabetes Mellitus, a chronic metabolic disorder characterized by hyperglycemia, has far-reaching implications beyond its primary effects on glucose metabolism. Recent research has shed light on the intricate relationship between diabetes and bone health, revealing significant negative effects on bone tissue biomechanics (Limirio et al., 2024).

The present study used an animal model. T1DM induction was done through intravenous administration of streptozotocin, based on the toxic effect of this drug on

pancreatic β cells, that induces a model of T1DM (Deeds et al., 2011) similar to that found in humans (Prabowo et al., 2014). The intravenous administration of streptozotocin is currently the most stable and similar model to reproduce the disease, with a low rate of reversal and mortality (Dias et al., 2018; Deeds et al., 2011).

The analysis of bone repair was performed using bi-dimensional histomorphometry in histological images (Batista et al., 2015; Dias et al., 2018) and three-dimensional using microcomputed tomography (Limirio et al., 2022). These methods together allowed a better evaluation of the bone repair process. In histological images, it was possible to evaluate the repair tissue qualitatively and quantitatively the production of bone matrix. Furthermore, MicroCT images allowed three-dimensional analysis of the bone matrix's constitution and the microarchitecture of this matrix at the repair site. The association of these analysis methods favored the analysis of the repair process in diabetics submitted to insulin therapy and HO allowing the evaluation of possible repercussions of these therapies on bone properties, after the repair was completed.

Trabecular thickness and trabecular separation are important indicators of bone structural health. A reduced Tb.Th and TB.Sp may indicate a weaker bone structure, while a higher Tb.Th and TB.Sp suggests a more robust and potentially more future resistant bone tissue (Limirio et al., 2024). Therefore, changes in trabecular thickness and trabecular separation caused by diabetes disease can impact future bone biomechanics by influencing load-bearing capacity and resistance to fractures. Cortical bone, responsible for providing structural support, may also be adversely affected, further compromising bone biomechanics (Limirio et al., 2024). In the present study, these parameters in the D and DH groups showed significant differences when compared with N, NH, DI, and DIH groups. These occur because T1DM causes a chronic inflammatory state, which can contribute to the impairment of bone turnover and repair, negatively impacting trabecular microarchitecture (Cipriani et al., 2020). Furthermore, T1DM causes decreased bone mineral density and bone formation and increased bone resorption (Salhotra et al., 2020). This leads to changes in the microarchitectural structure of bones, including a decrease in the number and thickness of trabecular (Limirio et al., 2024).

The groups submitted the oxygenation hyperbaric showed a higher formation of bone matrix compared with the other groups. Thereby demonstrating that the oxygenation

hyperbaric contributes to accelerated wound healing, because HO emerges as an intervention with potential positive effects on bone repair in diabetics post-surgery: enhanced oxygen supply, stimulation of angiogenesis (Mathieu et al., 2006), reduction of inflammation (Benson et al., 2003), antimicrobial properties, collagen synthesis and osteogenesis (Gajendrareddy et al., 2017), accelerated wound healing (Eldisoky et al., 2023; Thom, 2011; Dias 2018).

Furthermore, hyperbaric oxygenation has been shown to improve glycemic control by enhancing insulin sensitivity and glucose uptake in tissues. By creating a hyperoxic environment, HO helps mitigate the stress-induced hyperglycemic response, promoting glycemic normalization in diabetic patients (Prabowo et al., 2014). Groups NH, DH, and DIH showed a lower glucose level compared with the N, D, and DI, respectively. This suggests a potential for partial restoration of insulin-producing function, leading to decreased glucose levels and bringing diabetic individuals closer to normoglycemia (Prabowo et al., 2014).

Conclusion

The present study showed that association of insulin therapy and HO improved early bone regeneration in diabetic rats and proved to be an important treatment to minimize the deleterious effects of diabetes on bone regeneration, bringing them closer to normoglycemic rats.

References

1. Ay B, Parolia K, Liddell RS, Qiu Y, Grasselli G, Cooper DML, et al. Hyperglycemia compromises Rat Cortical Bone by Increasing Osteocyte Lacunar Density and Decreasing Vascular Canal Volume. *Commun Biol.* 2020;3(1):20.

2. Benson RM, Minter LM, Osborne BA, Granowitz EV. Hyperbaric oxygen inhibits stimulus-induced proinflammatory cytokine synthesis by human blood-derived monocyte-macrophages. *Clin Exp Immunol.* 2003;134(1):57-62.
3. Cipriani C, Colangelo L, Santori R, Renella M, Mastrantonio M, Minisola S, et al. The Interplay Between Bone and Glucose Metabolism. *Frontiers in endocrinology.* 2020;11:122.
4. Claes L, Recknagel S, Ignatius A. Fracture healing under healthy and inflammatory conditions. *Nature reviews Rheumatology.* 2012;8(3):133-43.
5. Claes L, Reusch M, Göckelmann M, Ohnmacht M, Wehner T, Amling M, et al. Metaphyseal fracture healing follows similar biomechanical rules as diaphyseal healing. *Journal of orthopaedic research : official publication of the Orthopaedic Research Society.* 2011;29(3):425-32.
6. Conte C, Epstein S, Napoli N. Insulin resistance and bone: a biological partnership. *Acta diabetologica.* 2018;55(4):305-14.
7. De Wolde SD, Hulskes RH, Weenink RP, Hollmann MW, Van Hulst RA. The Effects of Hyperbaric Oxygenation on Oxidative Stress, Inflammation and Angiogenesis. *Biomolecules.* 2021;11(8).
8. Dias PC, Limirio P, Linhares CRB, Bergamini ML, Rocha FS, Morais RB, et al. Hyperbaric Oxygen therapy effects on bone regeneration in Type 1 diabetes mellitus in rats. *Connect Tissue Res.* 2018;59(6):574-80.
9. Eldisoky RH, Younes SA, Omar SS, Gharib HS, Tamara TA. Hyperbaric oxygen therapy efficacy on mandibular defect regeneration in rats with diabetes mellitus: an animal study. *BMC Oral Health.* 2023;23(1):101.
10. Fulzele K, Riddle RC, DiGirolamo DJ, Cao X, Wan C, Chen D, et al. Insulin receptor signaling in osteoblasts regulates postnatal bone acquisition and body composition. *Cell.* 2010;142(2):309-19.
11. Gajendrareddy PK, Junges R, Cygan G, Zhao Y, Marucha PT, Engeland CG. Increased oxygen exposure alters collagen expression and tissue architecture during ligature-induced periodontitis. *J Periodontal Res.* 2017;52(3):644-9.
12. Izumino J, Kaku M, Yamamoto T, Yashima Y, Kagawa H, Ikeda K, et al. Effects of hyperbaric oxygen treatment on calvarial bone regeneration in young and adult mice. *Archives of oral biology.* 2020;117:104828.

13. Jan A, Sandor GK, Brkovic BB, Peel S, Evans AW, Clokie CM. Effect of hyperbaric oxygen on grafted and nongrafted calvarial critical-sized defects. *Oral Surg Oral Med Oral Pathol Oral Radiol Endod.* 2009;107(2):157-63.
14. Jiao H, Xiao E, Graves DT. Diabetes and Its Effect on Bone and Fracture Healing. *Current osteoporosis reports.* 2015;13(5):327-35.
15. Limirio P, da Rocha Junior HA, Morais RB, Hiraki KRN, Balbi APC, Soares PBF, et al. Influence of hyperbaric oxygen on biomechanics and structural bone matrix in type 1 diabetes mellitus rats. *PLoS One.* 2018;13(2):e0191694.
16. Limirio P, De Oliveira Neto NF, Venâncio JF, Linhares C, Soares PBF, Dechichi P. Insulin Therapy on Bone Macroscopic, Microarchitecture, and Mechanical Properties of Tibia in Diabetic Rats. *Current diabetes reviews.* 2024.
17. Martin ET, Kaye KS, Knott C, Nguyen H, Santarossa M, Evans R, et al. Diabetes and Risk of Surgical Site Infection: A Systematic Review and Meta-analysis. *Infection control and hospital epidemiology.* 2016;37(1):88-99.
18. Mathieu D, Favory R, Collet F, Linke J-C, Wattel F. Physiologic Effects of Hyperbaric Oxygen on Hemodynamics and Microcirculation. 2006. p. 75-101.
19. Prabowo S, Nataatmadja M, Hadi J, Dikman I, Handajani F, Ejt S, et al. Hyperbaric Oxygen Treatment in a Diabetic Rat Model Is Associated with a Decrease in Blood Glucose, Regression of Organ Damage and Improvement in Wound Healing. *Health.* 2014;06:1950-8.
20. Rubin MR. Skeletal fragility in diabetes. *Annals of the New York Academy of Sciences.* 2017;1402(1):18-30.
21. Saito M, Marumo K. Collagen cross-links as a determinant of bone quality: a possible explanation for bone fragility in aging, osteoporosis, and diabetes mellitus. *Osteoporos Int.* 2010;21(2):195-214.
22. Salhotra A, Shah HN, Levi B, Longaker MT. Mechanisms of bone development and repair. *Nat Rev Mol Cell Biol.* 2020;21(11):696-711.
23. Thom SR. Hyperbaric oxygen: its mechanisms and efficacy. *Plast Reconstr Surg.* 2011;127 Suppl 1(Suppl 1):131S-41S.
24. Thrailkill KM, Lumpkin CK, Bunn RC, Kemp SF, Fowlkes JL. Is insulin an anabolic agent in bone? Dissecting the diabetic bone for clues. *American Journal of Physiology-Endocrinology and Metabolism.* 2005;289(5):E735-E45.

25. Vashishth D. The role of the collagen matrix in skeletal fragility. *Current osteoporosis reports*. 2007;5(2):62-6.
26. Wongdee K, Krishnamra N, Charoenphandhu N. Derangement of calcium metabolism in diabetes mellitus: negative outcome from the synergy between impaired bone turnover and intestinal calcium absorption. *The Journal of Physiological Sciences*. 2017;67(1):71-81.

3 – CONCLUSÃO

Concluiu-se que o presente estudo mostrou que a terapia com oxigenação hiperbárica diminui os efeitos negativos da hiperglicemia em ratos diabéticos, melhorando a regeneração óssea. E de que o método automatizado oferece uma avaliação rápida e precisa, com potencial para reduzir o viés e padronizar a análise histológica, sugerindo que essa técnica pode ser utilizada de forma confiável para quantificação da matriz óssea.

4 – REFERÊNCIAS*

1. Aeimlapa R, Wongdee K, Charoenphandhu N, Suntornsaratoon P, Krishnamra N. Premature chondrocyte apoptosis and compensatory upregulation of chondroregulatory protein expression in the growth plate of Goto-Kakizaki diabetic rats. *Biochemical and biophysical research communications*. 2014;452(3):395-401.
2. Ay B, Parolia K, Liddell RS, Qiu Y, Grasselli G, Cooper DML, et al. Hyperglycemia compromises Rat Cortical Bone by Increasing Osteocyte Lacunar Density and Decreasing Vascular Canal Volume. *Commun Biol*. 2020;3(1):20.
3. Bao K, Jiao Y, Xing L, Zhang F, Tian F. The role of wnt signaling in diabetes-induced osteoporosis. *Diabetology & Metabolic Syndrome*. 2023;15(1):84.
4. Batista JD, Sargenti-Neto S, Dechichi P, Rocha FS, Pagnoncelli RM. Low-level laser therapy on bone repair: is there any effect outside the irradiated field? *Lasers Med Sci*. 2015;30(5):1569-74.
5. Benson RM, Minter LM, Osborne BA, Granowitz EV. Hyperbaric oxygen inhibits stimulus-induced proinflammatory cytokine synthesis by human blood-derived monocyte-macrophages. *Clin Exp Immunol*. 2003;134(1):57-62.
6. Cipriani C, Colangelo L, Santori R, Renella M, Mastrantonio M, Minisola S, et al. The Interplay Between Bone and Glucose Metabolism. *Frontiers in endocrinology*. 2020;11:122.
7. Claes L, Recknagel S, Ignatius A. Fracture healing under healthy and inflammatory conditions. *Nature reviews Rheumatology*. 2012;8(3):133-43.
8. Claes L, Reusch M, Göckelmann M, Ohnmacht M, Wehner T, Amling M, et al. Metaphyseal fracture healing follows similar biomechanical rules as diaphyseal healing. *Journal of orthopaedic research : official publication of the Orthopaedic Research Society*. 2011;29(3):425-32.

* De acordo com a Norma da FOUFU, baseado nas Normas de Vancouver. Abreviaturas dos periódicos com conformidade com Medline (Pubmed).

9. Deeds MC, Anderson JM, Armstrong AS, Gastineau DA, Hiddinga HJ, Jahangir A, et al. Single dose streptozotocin-induced diabetes: considerations for study design in islet transplantation models. *Laboratory animals*. 2011;45(3):131-40.
10. Dias PC, Limirio P, Linhares CRB, Bergamini ML, Rocha FS, Morais RB, et al. Hyperbaric Oxygen therapy effects on bone regeneration in Type 1 diabetes mellitus in rats. *Connect Tissue Res*. 2018;59(6):574-80.
11. Du JH, Lin SX, Wu XL, Yang SM, Cao LY, Zheng A, et al. The Function of Wnt Ligands on Osteocyte and Bone Remodeling. *J Dent Res*. 2019;98(8):930-8.
12. Eldisoky RH, Younes SA, Omar SS, Gharib HS, Tamara TA. Hyperbaric oxygen therapy efficacy on mandibular defect regeneration in rats with diabetes mellitus: an animal study. *BMC Oral Health*. 2023;23(1):101.
13. Gajendrareddy PK, Junges R, Cygan G, Zhao Y, Marucha PT, Engeland CG. Increased oxygen exposure alters collagen expression and tissue architecture during ligature-induced periodontitis. *J Periodontal Res*. 2017;52(3):644-9.
14. Goldman RJ. Hyperbaric oxygen therapy for wound healing and limb salvage: a systematic review. *PM R*. 2009;1(5):471-89.
15. Gonzalez RC, Woods RE. *Digital image processing*. New York, NY: Pearson; 2018. xvi, 1168 pages p.
16. Hammes J, Tager P, Drzezga A. EBONI: A Tool for Automated Quantification of Bone Metastasis Load in PSMA PET/CT. *J Nucl Med*. 2018;59(7):1070-5.
17. Jan A, Sandor GK, Brkovic BB, Peel S, Evans AW, Clokie CM. Effect of hyperbaric oxygen on grafted and nongrafted calvarial critical-sized defects. *Oral Surg Oral Med Oral Pathol Oral Radiol Endod*. 2009;107(2):157-63.
18. Jiao H, Xiao E, Graves DT. Diabetes and Its Effect on Bone and Fracture Healing. *Current osteoporosis reports*. 2015;13(5):327-35.
19. Jones TR, Carpenter AE, Lamprecht MR, Moffat J, Silver SJ, Grenier JK, et al. Scoring diverse cellular morphologies in image-based screens with iterative feedback and machine learning. *Proc Natl Acad Sci U S A*. 2009;106(6):1826-31.

20. Kawada S, Wada E, Matsuda R, Ishii N. Hyperbaric hyperoxia accelerates fracture healing in mice. *PLoS One*. 2013;8(8):e72603.
21. Kim JJ, Nam J, Jang IG. Fully automated segmentation of a hip joint using the patient-specific optimal thresholding and watershed algorithm. *Comput Methods Programs Biomed*. 2018;154:161-71.
22. Lamprecht MR, Sabatini DM, Carpenter AE. CellProfiler: free, versatile software for automated biological image analysis. *Biotechniques*. 2007;42(1):71-5.
23. Limirio P, da Rocha Junior HA, Morais RB, Hiraki KRN, Balbi APC, Soares PBF, et al. Influence of hyperbaric oxygen on biomechanics and structural bone matrix in type 1 diabetes mellitus rats. *PLoS One*. 2018;13(2):e0191694.
24. Limirio P, De Oliveira Neto NF, Venâncio JF, Linhares C, Soares PBF, Dechichi P. Insulin Therapy on Bone Macroscopic, Microarchitecture, and Mechanical Properties of Tibia in Diabetic Rats. *Current diabetes reviews*. 2024.
25. Limirio P, Soares PBF, Venancio JF, Rabelo GD, Soares CJ, Dechichi P. Type I Diabetes Mellitus and Insulin Therapy on Bone Microarchitecture, Composition and Mechanical Properties. *Current diabetes reviews*. 2022;18(8):e301121198427.
26. Linhares CRB, Rabelo GD, Limirio P, Venancio JF, Ribeiro Silva IG, Dechichi P. Automated bone healing evaluation: New approach to histomorphometric analysis. *Microsc Res Tech*. 2022;85(10):3339-46.
27. Martin ET, Kaye KS, Knott C, Nguyen H, Santarossa M, Evans R, et al. Diabetes and Risk of Surgical Site Infection: A Systematic Review and Meta-analysis. *Infection control and hospital epidemiology*. 2016;37(1):88-99.
28. Mathieu D, Favory R, Collet F, Linke J-C, Wattel F. Physiologic Effects of Hyperbaric Oxygen on Hemodynamics and Microcirculation. 2006. p. 75-101.
29. Mendes EM, Irie MS, Rabelo GD, Borges JS, Dechichi P, Diniz RS, et al. Effects of ionizing radiation on woven bone: influence on the osteocyte lacunar network, collagen maturation, and microarchitecture. *Clin Oral Investig*. 2020;24(8):2763-71.

30. Napoli N, Chandran M, Pierroz DD, Abrahamsen B, Schwartz AV, Ferrari SL, et al. Mechanisms of diabetes mellitus-induced bone fragility. *Nat Rev Endocrinol*. 2017;13(4):208-19.
31. Nyman JS, Even JL, Jo CH, Herbert EG, Murry MR, Cockrell GE, et al. Increasing duration of type 1 diabetes perturbs the strength-structure relationship and increases brittleness of bone. *Bone*. 2011;48(4):733-40.
32. Okubo Y, Bessho K, Fujimura K, Kusumoto K, Ogawa Y, Iizuka T. Effect of hyperbaric oxygenation on bone induced by recombinant human bone morphogenetic protein-2. *Br J Oral Maxillofac Surg*. 2001;39(2):91-5.
33. Palermo A, D'Onofrio L, Buzzetti R, Manfrini S, Napoli N. Pathophysiology of Bone Fragility in Patients with Diabetes. *Calcif Tissue Int*. 2017;100(2):122-32.
34. Prabowo S, Nataatmadja M, Hadi J, Dikman I, Handajani F, Ejt S, et al. Hyperbaric Oxygen Treatment in a Diabetic Rat Model Is Associated with a Decrease in Blood Glucose, Regression of Organ Damage and Improvement in Wound Healing. *Health*. 2014;06:1950-8.
35. Reyes-Fernandez PC, Periou B, Decrouy X, Relaix F, Authier FJ. Automated image-analysis method for the quantification of fiber morphometry and fiber type population in human skeletal muscle. *Skeletal Muscle*. 2019;9(1):15.
36. Rocha FS, Gomes Moura CC, Rocha Rodrigues DB, Zanetta-Barbosa D, Nakamura Hiraki KR, Dechichi P. Influence of hyperbaric oxygen on the initial stages of bone healing. *Oral Surg Oral Med Oral Pathol Oral Radiol*. 2015;120(5):581-7.
37. Rocha FS, Limirio PH, Zanetta-Barbosa D, Batista JD, Dechichi P. The effects of ionizing radiation on the growth plate in rat tibiae. *Microsc Res Tech*. 2016;79(12):1147-51.
38. Rubin MR. Skeletal fragility in diabetes. *Annals of the New York Academy of Sciences*. 2017;1402(1):18-30.
39. Saito M, Fujii K, Mori Y, Marumo K. Role of collagen enzymatic and glycation induced cross-links as a determinant of bone quality in spontaneously diabetic WBN/Kob rats. *Osteoporos Int*. 2006;17(10):1514-23.

40. Saito M, Marumo K. Collagen cross-links as a determinant of bone quality: a possible explanation for bone fragility in aging, osteoporosis, and diabetes mellitus. *Osteoporos Int.* 2010;21(2):195-214.
41. Saito M, Marumo K. Effects of Collagen Crosslinking on Bone Material Properties in Health and Disease. *Calcif Tissue Int.* 2015;97(3):242-61.
42. Salhotra A, Shah HN, Levi B, Longaker MT. Mechanisms of bone development and repair. *Nat Rev Mol Cell Biol.* 2020;21(11):696-711.
43. Schindelin J, Rueden CT, Hiner MC, Eliceiri KW. The ImageJ ecosystem: An open platform for biomedical image analysis. *Mol Reprod Dev.* 2015;82(7-8):518-29.
44. Sellmeyer DE, Civitelli R, Hofbauer LC, Khosla S, Lecka-Czernik B, Schwartz AV. Skeletal Metabolism, Fracture Risk, and Fracture Outcomes in Type 1 and Type 2 Diabetes. *Diabetes.* 2016;65(7):1757-66.
45. Silva A, Martins S, Neves L, de Faria P, Tosta T, Zanchetta do Nascimento M. Automated Nuclei Segmentation in Dysplastic Histopathological Oral Tissues Using Deep Neural Networks. 2019. p. 365-74.
46. Silva L, Figueira Venâncio J, Loures A, Lopes D, Dechichi P, Rabelo G. Efeito do Diabetes Mellitus tipo I na organização espacial das trabéculas ósseas: análise por meio do processo de esqueletonização. *HU Revista.* 2018;44:7.
47. Soares PBF, Soares CJ, Limirio P, de Jesus RNR, Dechichi P, Spin-Neto R, et al. Effect of ionizing radiation after-therapy interval on bone: histomorphometric and biomechanical characteristics. *Clin Oral Investig.* 2019;23(6):2785-93.
48. Starup-Linde J, Lykkeboe S, Gregersen S, Hauge E-M, Langdahl BL, Handberg A, et al. Bone Structure and Predictors of Fracture in Type 1 and Type 2 Diabetes. *The Journal of Clinical Endocrinology & Metabolism.* 2016;101(3):928-36.
49. Steiner DF, MacDonald R, Liu Y, Truszkowski P, Hipp JD, Gammage C, et al. Impact of Deep Learning Assistance on the Histopathologic Review of Lymph Nodes for Metastatic Breast Cancer. *Am J Surg Pathol.* 2018;42(12):1636-46.

50. Suzuki M, Urai S, Fukuoka H, Hirota Y, Yamamoto M, Okada Y, et al. Relation between the insulin lowering rate and changes in bone mineral density: Analysis among subtypes of type 1 diabetes mellitus. 2022;13(9):1585-95.
51. Tamminga GG, Paulitsch-Fuchs AH, Jansen GJ, Euverink GW. Different binarization processes validated against manual counts of fluorescent bacterial cells. *J Microbiol Methods*. 2016;128:118-24.
52. Thom SR. Hyperbaric oxygen: its mechanisms and efficacy. *Plast Reconstr Surg*. 2011;127 Suppl 1(Suppl 1):131S-41S.
53. Thrailkill KM, Lumpkin CK, Jr., Bunn RC, Kemp SF, Fowlkes JL. Is insulin an anabolic agent in bone? Dissecting the diabetic bone for clues. *Am J Physiol Endocrinol Metab*. 2005;289(5):E735-45.
54. Vashishth D. The role of the collagen matrix in skeletal fragility. *Current osteoporosis reports*. 2007;5(2):62-6.
55. Wang J, Wang B, Li Y, Wang D, Lingling E, Bai Y, et al. High glucose inhibits osteogenic differentiation through the BMP signaling pathway in bone mesenchymal stem cells in mice. *EXCLI journal*. 2013;12:584-97.
56. Wang S, Yang DM, Rong R, Zhan X, Xiao G. Pathology Image Analysis Using Segmentation Deep Learning Algorithms. *Am J Pathol*. 2019;189(9):1686-98.
57. Wang X, Liu L, Zhang W, Zhang J, Du X, Huang Q, et al. Serum metabolome biomarkers associate low-level environmental perfluorinated compound exposure with oxidative /nitrosative stress in humans. *Environ Pollut*. 2017;229:168-76.
58. Wijenayaka AR, Kogawa M, Lim HP, Bonewald LF, Findlay DM, Atkins GJ. Sclerostin stimulates osteocyte support of osteoclast activity by a RANKL-dependent pathway. *PLoS One*. 2011;6(10):e25900.
59. Wu D, Malda J, Crawford R, Xiao Y. Effects of hyperbaric oxygen on proliferation and differentiation of osteoblasts from human alveolar bone. *Connect Tissue Res*. 2007;48(4):206-13.

60. Yang X, Gandhi C, Rahman MDM, Appleford M, Sun L-W, Wang X. Age-Related Effects of Advanced Glycation End Products (Ages) in Bone Matrix on Osteoclastic Resorption. *Calcified Tissue International*. 2015;97(6):592-601.

5 – ANEXOS

1 – Certificado do parecer de ética em utilização de animais



Universidade Federal de Uberlândia
– Comissão de Ética na Utilização de Animais –



CERTIFICADO

Certificamos que o protocolo para uso de animais em experimentação nº 026/14, sobre o projeto de pesquisa intitulado "Efeito da oxigenação hiperbárica e do laser de baixa potência no reparo e biomecânica em osso de ratos diabéticos", sob a responsabilidade da **Profª. Drª. Paula Dechichi** está de acordo com os princípios éticos na experimentação animal conforme regulamentações do Conselho Nacional de Controle e Experimentação Animal (CONCEA) e foi **APROVADO** pela Comissão de Ética na Utilização de Animais (CEUA) – UFU em reunião de **29 de Agosto de 2014**.

(We certify that the protocol nº 026/14, about "Efeito da oxigenação hiperbárica e do laser de baixa potência no reparo e biomecânica em osso de ratos diabéticos", agrees with the ETHICAL PRINCIPLES ON ANIMAL RESEARCH as regulations of National Advice of Control and Animal Experimentation (CONCEA) and approved by Ethics Commission on Use of Animals (CEUA) – Federal University of Uberlândia in 29/08/2014).

Uberlândia, 29 de Agosto de 2014.



Prof. Dr. César Augusto Garcia
Coordenador da CEUA/UFU